HHS Public Access

Author manuscript

Brain Behav Immun. Author manuscript; available in PMC 2019 May 30.

Published in final edited form as:

Brain Behav Immun. 2019 January ; 75: 72–83. doi:10.1016/j.bbi.2018.09.018.

Brain glial activation in fibromyalgia - a multi-site positron emission tomography investigation

Daniel S. Albrecht[a,*], **Anton Forsberg**[b,*], **Angelica Sandstrom**[c,d], **Courtney Bergan**[a], **Diana Kadetoff**[c,d,e], **Ekaterina Protsenko**[a], **Jon Lampa**[f], **Yvonne C. Lee**[g,h], **Caroline Olgart Höglund**[i], **Ciprian Catana**[a], **Simon Cervenka**[b], **Oluwaseun Akeju**[j], **Mats Lekander**[c,d,k], **George Cohen**[l], **Christer Halldin**, **Norman Taylor**, **Minhae Kim**, **Jacob M. Hooker**, **Robert R. Edwards**, **Vitaly Napadow**[a,m], **Eva Kosek**[c,d,e,‡], and **Marco L. Loggia**[a,‡]

[a]A. A. Martinos Center for Biomedical Imaging, Department of Radiology, Massachusetts General Hospital, Harvard Medical School, Boston, MA, United States

[b]Department of Clinical Neuroscience, Center for Psychiatry Research, Karolinska Institutet, and Stockholm County Council, SE-171 76 Stockholm, Sweden

[c]Department of Clinical Neuroscience, Karolinska Institutet, Stockholm, Sweden

[d]Department of Neuroradiology, Karolinska University Hospital, Stockholm, Sweden

[e]Stockholm Spine Center, Stockholm, Sweden.

[f]Rheumatology Unit, Department of Medicine, Karolinska Institutet, Karolinska University Hospital, Stockholm, Sweden

[g]Division of Rheumatology, Brigham and Women's Hospital, Harvard Medical School, Boston, MA, United States

[h]Division of Rheumatology, Northwestern University Feinberg School of Medicine, Chicago, IL, United States

[i]Department of Physiology and Pharmacology, Karolinska Institutet, Stockholm, Sweden

[j]Department of Anesthesia, Critical Care and Pain Medicine, Massachusetts General Hospital, Harvard Medical School, Boston, MA, United States

[k]Stress Research Institute, Stockholm University, Stockholm, Sweden

[l]Department of Rheumatology, Massachusetts General Hospital, Harvard Medical School, Boston, MA, United States

[m]Department of Anesthesiology, Brigham and Women's Hospital, Harvard Medical School, Boston, MA, United States

Correspondence to: Marco L. Loggia, PhD, A. A. Martinos Center for Biomedical Imaging, Massachusetts General Hospital, 149 Thirteenth Street, Room 2301, Charlestown, MA 02129, marco.loggia@mgh.harvard.edu, Eva Kosek, M.D., PhD, Department of Clinical, Neuroscience, Karolinska Institutet, Nobels väg 9, 171 77 Stockholm, Sweden, Eva.Kosek@ki.se.

*Co-first author;

‡Co-senior author

All authors report no conflicts of interest

Abstract

Fibromyalgia (FM) is a poorly understood chronic condition characterized by widespread musculoskeletal pain, fatigue, and cognitive difficulties. While mounting evidence suggests a role for neuroinflammation, no study has directly provided evidence of brain glial activation in FM. In this study, we conducted a Positron Emission Tomography (PET) study using [^{11}C]PBR28, which binds to the translocator protein (TSPO), a protein upregulated in activated microglia and astrocytes. To enhance statistical power and generalizability, we combined datasets collected independently at two separate institutions (Massachusetts General Hospital [MGH] and Karolinska Institutet [KI]). In an attempt to disentangle the contributions of different glial cell types to FM, a smaller sample was scanned at KI with [^{11}C]-$_{L}$-deprenyl-D_2 PET, thought to primarily reflect astrocytic (but not microglial) signal.

Thirty-one FM patients and 27 healthy controls (HC) were examined using [^{11}C]PBR28 PET. 11 FM patients and 11 HC were scanned using [^{11}C]-$_{L}$-deprenyl-D_2 PET. Standardized uptake values normalized by occipital cortex signal (SUVR) and distribution volume (V_T) were computed from the [^{11}C]PBR28 data. [^{11}C]-$_{L}$-deprenyl-D_2 was quantified using λk_3. PET imaging metrics were compared across groups, and when differing across groups, against clinical variables.

Compared to HC, FM patients demonstrated widespread cortical elevations, and no decreases, in [^{11}C]PBR28 V_T and SUVR, most pronounced in the medial and lateral walls of the frontal and parietal lobes. No regions showed significant group differences in [^{11}C]-$_{L}$-deprenyl-D_2 signal, including those demonstrating elevated [^{11}C]PBR28 signal in patients (p's≥0.53, uncorrected). The elevations in [^{11}C]PBR28 V_T and SUVR were correlated both spatially (i.e., were observed in overlapping regions) and, in several areas, also in terms of magnitude. In exploratory, uncorrected analyses, higher subjective ratings of fatigue in FM patients were associated with higher [^{11}C]PBR28 SUVR in the anterior and posterior middle cingulate cortices (p's<0.03). SUVR was not significantly associated with any other clinical variable.

Our work provides the first *in vivo* evidence supporting a role for glial activation in FM pathophysiology. Given that the elevations in [^{11}C]PBR28 signal were not also accompanied by increased [^{11}C]-$_{L}$-deprenyl-D_2 signal, our data suggests that microglia, but not astrocytes, may be driving the TSPO elevation in these regions. Although [^{11}C]-$_{L}$-deprenyl-D_2 signal was not found to be increased in FM patients, larger studies are needed to further assess the role of possible astrocytic contributions in FM. Overall, our data support glial modulation as a potential therapeutic strategy for FM.

Keywords

Fibromyalgia; Positron emission tomography; neuroinflammation; microglia; astrocytes; functional pain; TSPO; chronic overlapping pain conditions; neuroimmunology; MRI/PET; Deprenyl-D2

1. INTRODUCTION

Fibromyalgia (FM) is a poorly understood chronic condition characterized by widespread musculoskeletal pain, fatigue, unrefreshing sleep, memory and attention difficulties, among

other symptoms (Clauw, 2014). While the etiology of FM is unknown, central mechanisms are strongly implicated, including evidence of abnormalities in structure, function, and molecular chemistry of the central nervous system (CNS) (Albrecht et al., 2016; Clauw, 2014; Dehghan et al., 2016; Flodin et al., 2014; Gracely et al., 2002; Harris et al., 2007; Jensen et al., 2009; Jensen et al., 2010; Jensen et al., 2013; Kuchinad et al., 2007; Loggia et al., 2014; Loggia et al., 2015a; Napadow and Harris, 2014; Schreiber et al., 2017; Schrepf et al., 2016; Wood, 2008), though some evidence points to peripheral alterations as well (Oaklander et al., 2013; Uceyler and Sommer, 2013).

Dysregulation of neuroimmune activation is one potential mechanism contributing to previously reported central aberrations and central sensitization in FM. For instance, FM patients demonstrate elevated levels of fractalkine and interleukin-8 (IL-8) in cerebrospinal fluid (CSF) (Backryd et al., 2017; Kadetoff et al., 2012; Kosek et al., 2015). Both chemokines are implicated in neuron-glial communication (Montague and Malcangio, 2017; Puma et al., 2001), and have been associated with central sensitization and pain (Kosek et al., 2015; Montague and Malcangio, 2017). However, no study to date has clearly demonstrated that glial activation occurs in the brain of FM patients. Acknowledging a role for neuroimmune dysfunction in FM would open the exploration of glial modulation as a therapeutic option for this condition.

In the human CNS, glial activation can be studied *in vivo* using positron emission tomography (PET) and radioligands that bind to the 18-kDa translocator protein (TSPO), such as [^{11}C]PBR28, which displays nanomolar affinity to this protein (~0.5nM; Imaizumi et al., 2008). Located mainly on the outer mitochondrial membrane, TSPO expression is low in healthy CNS tissue, but is widely upregulated in microglia and astrocytes under inflammatory conditions (Lavisse et al., 2012; Rupprecht et al., 2010). Our group has recently used TSPO PET imaging to document neuroimmune activation in the central and peripheral nervous system of patients with chronic low back pain (CLBP) (Albrecht et al., 2018; Loggia et al., 2015b). While no TSPO PET studies of FM patients have been published yet, a possible link between TSPO and FM pathophysiology is provided by an association between the Ala147Thr polymorphism (rs6971) in the *TSPO* gene and FM symptom severity and cerebral pain processing (Kosek et al., 2016).

The aims of the current study were to evaluate the hypothesis that brain TSPO binding in FM patients, as assessed using the [^{11}C]PBR28 PET ligand, is 1) elevated compared to healthy controls (indicating the presence of glial activation) and 2) correlated with specific symptoms attributable to FM pathophysiology. An additional third aim was to tease out the most likely cellular sources of increased TSPO binding because, while TSPO upregulation in neuroinflammatory responses consistently colocalizes with microglia, an accompanying astrocytic component has been observed in some (Liu et al., 2016; Rupprecht et al., 2010; Toth et al., 2016; Wei et al., 2013), but not all cases (Abourbeh et al., 2012; Mirzaei et al., 2016). To this end, a smaller sample of FM patients received a PET scan with [^{11}C]-$_{L}$-deprenyl-D_2, which binds to monoamine oxidase B (MAO-B) with high specificity in postmortem tissue (~30 fmol/mg tissue; Gulyas et al., 2011). Because the expression of MAO-B in glial cells is thought to be predominantly, if not exclusively, within astrocytes (Ekblom et al., 1994), we reasoned that the presence of elevations in [^{11}C]-$_{L}$-deprenyl-D_2

signal within regions also demonstrating TSPO elevations would support the presence of an astrocytic contribution to the TSPO signal. Conversely, the absence of [^{11}C]-$_{L}$-deprenyl-D_2 in regions showing elevated TSPO signal would suggest a predominantly microglial cellular source.

2. MATERIALS AND METHODS

2.1 Study Design

This collaborative project combines data from two independent research centers to amass a [^{11}C]PBR28 PET imaging cohort of FM patients and matched healthy controls (HC): Massachusetts General Hospital (MGH) in Boston, MA, United States, and Karolinska Institutet (KI) in Stockholm, Sweden. Both studies were approved by ethical commitees (MGH – Partners Human Research Committee; KI – Regional Ethical Review Board in Stockholm), and all subjects provided informed consent. The initial study design and data collection at each site were completed independently, and the decision to aggregate the data into a common analysis was made after completion of data collection. Potential confounds attributable to site-specific differences were taken into account in the statistical models of the combined dataset. Group differences identified in the primary analysis of the combined dataset were also assessed within each site separately. Because arterial plasma data were collected for all subjects scanned at Karolinska, we decided to perform two levels of analyses. The first analysis took advantage of the arterial blood data collected at Karolinska, in order to obtain quantitative distribution volume (V_T) metrics using kinetic modeling. The second analysis employed a blood-free ratio approach previously validated in separate cohorts (Albrecht et al., 2017), and utilized the enhanced statistical power of the combined sample (31 patients vs. 27 controls). An evaluation of the agreement between V_T computed in the smaller (KI only) sample and SUVR in the larger, combined sample (KI+MGH) was perfomed by assessing the extent of spatial overlap of the group differences, as well as the regional correlation of these metrics.

2.2 Subjects

In total, 31 FM patients (29 female, 50.7±11 y/o) and 27 controls (25 female, 49.4±11 y/o) received a [^{11}C]PBR28 PET brain scan. A total of 11 FM patients (11 female, 51.5±8.2 y/o), and 11 controls (11 female, 51.0±7.0 y/o) received a [^{11}C]-$_{L}$-deprenyl-D_2 brain scan. All FM patients had received a diagnosis of FM from a physician, and met the 2011 modifications of the American College of Rheumatology classification criteria for fibromyalgia (Wolfe et al., 2011). FM patients were excluded for the presence of any pain conditions other than FM. Exclusionary criteria for all subjects at either site included: history of major psychiatric illness, neurological illness, cardiovascular disease, inability to communicate in English (MGH) or Swedish (KI), and contraindication for PET/MR scanning (e.g., pacemaker, metallic implants, pregnancy, etc). Addtionally, at MGH, the use of benzodiazepine medications was exclusionary, except for clonazepam, alprazolam, and lorazepam, that show negligible binding to TSPO *in vitro*, even at large clinical doses (Canat et al., 1993; Clow et al., 1985; Gehlert et al., 1985; Kalk et al., 2013; Wamsley et al., 1993). At KI, benzodiazepines were not exclusionary, however no patients reported benzodiazepine

use (see Results). Please see Supplementary Table 1 for a detailed list of exclusion criteria by site.

2.2.1 Karolinska Institutet.—Eleven patients diagnosed with FM (11 female, 51.8±8,6 y/o) and 11 HC (11 female, 51.5±9.0 y/o) were matched according to age, sex and genotype for the Ala147Thr *TSPO* polymorphism (rs6971) which affects binding of TSPO radioligands, including [^{11}C]PBR28, both *in vitro* and *in vivo* (Collste et al., 2016; Kreisl et al., 2013a; Owen et al., 2010; Owen et al., 2012). Sixteen subjects were Ala/Ala (i.e., high-affinity binders;;HABs: FM n=8; HC n=8) and six were Ala/Thr (i.e., mixed-affinity binders; MABs: FM n=3; HC n=3). No Thr/Thr (i.e., low-affinity binders; LABs) were included. Eleven FM patients and 11 HC received a brain [^{11}C]PBR28 PET scan. Moreover, six of the 11 FM patients that completed the [^{11}C]PBR28 scan and agreed to participate in an additional PET scan, as well as five additional FM patients and 11 sex and age-matched healthy controls not previously examined, received a [^{11}C]-$_{L}$-deprenyl-D_2 PET scan. In addition to meeting 2011 ACR diagnostic criteria, all patients in the KI cohort also met the ACR 1990 criteria (Wolfe et al., 1990).

2.2.2 Massachusetts General Hospital.—Twenty patients diagnosed with FM (18 female, 48.0±1.2 y/o) were group matched with 16 HC subjects (14 female, 50.2±13 y/o) according to age, sex, and *TSPO* polymorphism. Twenty-four subjects were HABs (FM n=14; HC n=10), and 12 were MABs (FM n=6; HC n=6). No LABs were included in the study. At the MGH site, one patient also had chronic hepatitis C, one had idiopathic CD8 lymphocytopenia, and one had Meniere's Disease and diabetes. These subjects were not outliers on any of the PET imaging measures, and results were unaffected if these subjects were excluded.

2.3 Clinical Assessment

All FM patients completed the following clinical questionnaires: 2011 American College of Rheumatology self-report survey for the assessment of FM (ACR; Wolfe et al., 2011), FM Impact Questionnaire (FIQ; Bennett et al., 2009), Beck Depression Inventory (BDI; Beck et al., 1961), and Pain Catastrophizing Scale (PCS; Sullivan et al., 1995). All items were completed on the day of the scan, with the exception of the ACR survey for all KI patients and two MGH patients, and the BDI for MGH patients, which were completed only during the screening visit. Because 17 MGH patients completed the ACR survey on both the scan day and during the screening visit, we were able to confirm that this questionnaire has good temporal stability by correlating the scores across visits. All subscales of the ACR survey showed high to moderate intercorrelations (total: r=0.785, p<0.001; symptom severity: r=0.788, p<0.001; widespread pain index: r=0.728, p=0.001; fatigue: r=0.534, p=0.027; trouble thinking: r=0.581, p=0.015; waking up tired: r=0.810, p<0.001), supporting the temporal stability of these measures, and therefore the appropriateness of evaluating these variables in relation to imaging metrics collected at different timepoints.

Prior to tracer injection on the scan day, all patients also rated their pain on a visual analog scale, anchored by 0 ("No pain at all") and 100 ("Most intense pain tolerable").

2.4 Positron Emission Tomography (PET) and Magnestic Resonance (MR) Imaging

2.4.1 Karolinska Institutet.—PET imaging was performed using the High-Resolution Research Tomograph (Siemens Molecular Imaging, Knoxville, TN, USA) at the PET centre at Karolinska Institutet, Stockholm, Sweden. Structural MR images were collected using a 1.5-T Siemens Avanto scanner at Medicinsk Röntgen at Odenplan prior to the first PET scan (TR=1790 or 1800ms, TE=3.53 or 2.8ms, flip angle=15° or 8°, voxel size=1mm isotropic). Prior to PET scanning, subjects received a cubital vein catheter for intravenous radioligand administration and a radial artery catheter in the contralateral arm for arterial blood sampling. To minimize motion during the PET data acquisition, each participant wore an individually-designed helmet, placed in a frame holder.

Preparation, injection and PET data acquisition for [^{11}C]PBR28 have been described previously (Collste et al., 2016; Kanegawa et al., 2016). Average administered radioactivity of [^{11}C]PBR28 (MBq) was – HC: 416±40 (mean±SD), FM: 385±71; average specific radioactivity (GBq/μmol) – HC: 306±195, FM: 239±74; average injected mass (μg) – HC: 0.60±0.34, FM: 0.61±0.21. Average administered radioactivity of [^{11}C]-$_{L}$-deprenyl-D_2 was – HC: 364±46, FM: 366±45; average specific radioactivity – HC: 193±105, FM: 213±82 ; average injected mass – HC: 0.48±0.30, FM: 0.36±0.13. PET data were acquired for 63 minutes both for [^{11}C]PBR28 and [^{11}C]-$_{L}$-deprenyl-D_2. Manual samples were drawn at 2, 4, 6, 8, 10, 15, 20, 25, 30, 45, and 60 minutes for [^{11}C]PBR28 and 1, 2, 4, 6, 8, 10, 16, 20, 30, 40, and 60 minutes for [^{11}C]-$_{L}$-deprenyl-D_2. For one control subject in the [^{11}C]-$_{L}$-deprenyl-D_2 dataset, there was a technical issue with the arterial blood collection, and thus this subject was excluded from the analysis. Arterial blood data pre-processing was performed using Kaleidagraph 4.1 software (Synergy Software) as described previously (Collste et al., 2016). Radioligand metabolism correction was performed using the parent fraction in PMOD v3.3 (pixel-wise modelling software; PMOD Technologies Ltd., Zurich, Switzerland) where individual parent fraction data was fit with a 3-exponential model.

2.4.2 Massachusetts General Hospital.—Imaging was performed at the MGH/HST Athinoula A. Martinos Center for Biomedical Imaging in Charlestown, MA. [^{11}C]PBR28 was produced in-house using a procedure modified from the literature (Imaizumi et al., 2007). [^{11}C]PBR28 scans were performed for 90 minutes with an integrated PET/MR scanner consisting of a dedicated brain avalanche photodiode-based PET scanner in the bore of a Siemens 3T Tim Trio MRI (Kolb et al., 2012). A multi-echo MPRAGE volume was acquired prior to tracer injection (TR/TE1/TE2/TE3/TE4=2530/1.64/3.5/5.36/7.22 ms, flip angle=7°, voxel size=1mm isotropic) for the purpose of anatomical localization, spatial normalization of the imaging data, as well as generation of attenuation correction maps (Izquierdo-Garcia et al., 2014). Average administered radioactivity of [^{11}C]PBR28 (MBq) was – HC: 457±57 MBq, FM: 505±40; average specific activity (GBq/μmol) – HC: 77.4±30, FM: 71.8±26; average injected mass (μg) – HC: 2.32±0.8, FM: 2.78±1.1.

2.5 PET Data Analysis and Quantification

2.5.1 Kinetic analysis.—Estimation of [^{11}C]PBR28 distribution volume (V_T) was performed using Logan graphical analysis with a metabolite corrected plasma input function (Logan et al., 1990), based on five frames from 33 to 63 minutes. For each PET scan, a

parametric V_T image was generated using the stationary wavelet aided parametric imaging (WAPI) approach (Cselenyi et al., 2002). WAPI analysis of TSPO binding has been previously shown to be sensitive to within-subject changes in V_T (Forsberg et al., 2017; Jucaite et al., 2015), and has shown both high correlation with V_T estimated with the two-tissue compartment model (2TCM), and good reliability for 63 minutes of data (Collste et al., 2016).

Quantification of [^{11}C]-$_L$-deprenyl-D_2 data was performed as described previously, utilizing the 2TCM with three rate constants (K_1, k_2, k_3) with PMOD 3.3 (Sturm et al., 2017). The outcome measure λk_3 was calculated as $(K_1/k_2)*k_3$ which has been shown to reflect the regional enzyme concentration more accurately than k_3 alone (Fowler et al., 1995; Logan et al., 2000). There is presently no validated method to produce λk_3 parametric images with the WAPI methodology we used for the [^{11}C]PBR28 analysis. For this reason, [^{11}C]-$_L$-deprenyl-D_2 data was analyzed only using a region-of-interest (ROI) approach. Because an aim of this project was to assess the presence of a possible astrocytic component to TSPO signal in FM, the regions identified as statistically different across groups in the [^{11}C]PBR28 voxel-wise SUVR analyses (see below) were selected as ROIs. Addtionally, λk_3 values were computed for 23 anatomically defintied ROIs from the AAL atlas, whole brain, and whole gray matter for exploratory analyses.

2.5.2 SUVR analysis.—Static [^{11}C]PBR28 PET images were reconstructed from 33–63 minutes post-injection PET data, the latest 30-minute period available at both sites. Standardized uptake value (SUV) images were calculated by normalizing images by injected dose/body weight. SUV ratio images (SUVR) were obtained via normalization by PET signal from a pseudo-reference region (i.e., occipital cortex, identified using the occipital cortex label from the AAL atlas available in PMOD (Tzourio-Mazoyer et al., 2002)). We have previously utilized this approach for quantification of [^{11}C]PBR28 PET data in both chronic low back pain patients and in patients with ALS (Albrecht et al., 2017), showing that group differences in SUVR (in the thalamus and motor cortex, in pain and ALS patients, respectively) can be similarly observed using V_T (or V_T ratio; DVR) estimated with 2TCM, and that SUVR and DVR are strongly correlated. However, since some medial portions of the occipital cortex exhibited group differences in the V_T analysis (see Results), these were excluded from the occipital pseudo-reference region. A general linear model (GLM) analysis with genotype and injected dose as regressors of no interest, revealed that the mean SUV extracted from the occipital region defined above did not show any significant effects of Group ($F_{1,52}=4.38\times10^{-6}$, $p=0.99$), Site ($F_{1,52}=0.006$, $p=0.72$), or a Group*Site interaction ($F_{1,52}=0.08$, $p=0.20$). These results support the appropriateness of using this region as a pseudo-reference in this particular study.

2.5.3 Image Post-processing.—For both SUVR and V_T images, FSL and Freesurfer tools were used for image processing. PET images were co-registered to individual structural T1 images, normalized to MNI standard space, and spatially smoothed with an 8mm FWHM Gaussian kernel, as in Loggia et al., (2015b) and Albrecht et al., (2017).

2.6 Statistical analysis

Differences in continuous variables were assessed by performing a GLM analysis with Group and Site as fixed factors, and a Group*Site interaction term. Significant interaction terms were decomposed with post-hoc planned comparisons of least squares means. Differences in the distribution of categorical variables were assessed with Chi-Square tests. Between-site differences in FM questionnaire scores were assessed with two-sample t-tests.

As the primary analysis, voxelwise group comparisons of [^{11}C]PBR28 V_T and SUVR maps were performed with FSL's FEAT GLM tool (www.fmrib.ox.ac.uk/fsl, version 5.0.7), using a voxelwise cluster-forming threshold of z>2.3 and a (corrected) cluster significance threshold of $p<0.05$ to correct for multiple comparisons. *TSPO* polymorphism (Ala/Ala, Ala/Thr), was included as a regressor of no interest in both analyses. Study site (MGH, KI) was included as an additional regressor of no interest in SUVR analysis, as this was perfomed on the combined sample from both institutions. Because there was a statistically significant effect of Site ($F_{1,54}=37.9$, $p<0.001$) and a significant Group*Site interaction for injected dose ($F_{1,54}=4.23$, $p=0.044$), this variable was also added as a covariate of no interest in all group analyses using the combined dataset (KI+MGH). There were also significant effects of Site for specific activity and injected mass, but no significant Group*Site interactions. Therefore, we performed supplementary voxelwise analyses including these variables as regressors of no interest, in order to ensure that including them in the statistical model had negligible effects on the outcomes. Because no subcortical effects were detected, and for ease of visualization, imaging results were visualized on a surface (FreeSurfer's fsaverage).

For follow up analyses and illustration purposes, clusters of significant group differences from the SUVR or V_T analysis (Figs 1–3) were parcellated into separate anatomically-constrained subregions, using the labels from the Harvard-Oxford probabilistic atlas (using an arbitrary threshold of 30). Average SUVR and/or V_T values were extracted from these regions, for the purposes of visualizing data, comparing group effects within each site independently, and assessing relationships between SUVR and clinical variables and between outcome metrics (SUVR and V_T). Although anterior middle cingulate (aMCC) did not exhibit significant group differences in the voxelwise V_T analysis, this region was significant in the SUVR analysis (see Results); therefore, average V_T was extracted from aMCC to test for potential V_T differences not detected in the voxelwise analysis, particularly because this region is highly relevant to pain processing (Kragel et al., 2018; Shackman et al., 2011). Partial correlation analyses were used to assess correlations between PET signal extracted from regions exhibiting significant group differences in the voxelwise analyses and continuous clinical variables (i.e. ACR [total score, symptom severity score, widespread pain index], FIQR, BDI, PCS, and current VAS pain), correcting for *TSPO* polymorphism. These analyses were performed using SUVR, as these values were available for all patients at both sites. To assess the relationship between extracted PET signal and ordinal clinical variables (individual ACR symptom severity items: "fatigue", "trouble thinking or remembering", "waking up tired"), we performed GLM analyses with TSPO PET signal as the dependent variable, clinical score as a fixed factor ("slight or mild problem", "moderate problem", or "severe problem"), and *TSPO* polymorphism and study site as regressors of no interest.

Post-hoc planned comparisons of least squares means were performed to decompose significant main effects. Additionally, partial correlation analysis was used to evaluate the association between [^{11}C]PBR28 V_T and SUVR in participants for whom both measures were available, correcting for *TSPO* polymorphism.

After identifying regions demonstrating group differences in the combined [^{11}C]PBR28 SUVR datasets, we conducted a follow up GLM analysis of the data extracted from the same regions, in order to evaluate the significance of the Site effect and the Group*Site interaction, using *TSPO* genotype and injected dose as regressors of no interest, and to compute the effect size, using Cohen's *d*, for each site independently. The primary aim of these analyses was to assess whether the group differences identified in the voxelwise analyses were driven solely by one site, or could rather be similarly observed at both sites. In order to avoid circularity, we do not report the p-values for the Group effects at each site independently, as these analyses were performed on data extracted from regions preselected because they already exhibited a Group effect in the voxelwise analyses. For all demographic, correlation, and follow-up analyses, significance was set as $p<0.05$, uncorrected.

Unpaired t-tests were used to assess group differences in [^{11}C]-$_L$-deprenyl-D_2 λk_3 for each region with elevated TSPO signal, which included: aMCC, dLPFC, dmPFC, frontoinsular cortex, S1/M1, PCC, precuneus, pMCC, SMA, and SPL (see Results). Unpaired t-tests were also performed for the exploratory analysis of 23 anatomically define ROIs, and whole brain and gray matter. However, because no group differences were significant in any ROI, all analyses were followed up by exploratory uncorrected analyses to provide more convincing support to the claim that the lack of group effects reported in the deprenyl analyses are likely to reflect the lack of astrocytic activation in FM.

Please refer to Supplementary Table 2 for a summary of the statistical analyses.

3. RESULTS

3.1 Subject characteristics

Demographic and other key characteristics for all subjects are shown in Table 1. FM patients had significantly higher BMI than controls in the MGH dataset ($p<0.001$), but there were no significant patient-control differences for any other variable ($p's\geq0.071$) for any dataset. Clinical characteristics of all FM patients are presented in Table 2. For the [^{11}C]PBR28 analysis, FM patients from the KI site had significantly higher scores than FM patients from the MGH site on several of the ACR 2011 items ($p<0.047$; Table 2). KI patients included in both the [^{11}C]PBR28 and the [^{11}C]-$_L$-deprenyl-D_2 analyses were also less medicated (Table 3). There were no significant differences between FM patients at the KI site in the [^{11}C]PBR28 and [^{11}C]-$_L$-deprenyl-D_2 datasets for any demographic characteristic or clinical measure evaluated ($p's\geq0.29$).

3.2 [^{11}C]PBR28 analyses: Group differences

3.2.1 [^{11}C]PBR28 V_T comparison (KI sample only).—

In FM patients, [^{11}C]PBR28 V_T was elevated in several brain regions compared to healthy control subjects (Fig. 1),

including dorsolateral prefrontal cortex (dlPFC), dorsomedial PFC (dmPFC), primary somatosensory and motor cortices (S1/M1), precuneus, posterior cingulate cortex (PCC), supplementary motor area (SMA), supramarginal gyrus (SMG), and superior parietal lobule (SPL). Additionally, an ROI analysis of the aMCC revealed elevated V_T in the FM patients that approached statistical significance (p=0.071). There were no regions where control V_T was significantly higher than FM V_T.

3.2.2 [^{11}C]PBR28 SUVR comparison (KI + MGH).—

A whole brain voxelwise analysis identified several brain regions where SUVR in FM patients was significantly greater than in HC (Fig. 2). These regions largely overlapped those identified in the V_T analysis (dlPFC, dmPFC, S1/M1, precuneus, PCC, SMA, SPL) but also revealed effects in additional regions (aMCC, posterior MCC [pMCC], and frontoinsular cortex). There were no regions where SUVR was significantly higher in healthy controls relative to FM patients. Supplementary voxelwise analyses, including specific activity and injected mass as regressors of no interest, showed similar outcomes to the primary analysis, which included injected dose as a regressor of no interest (Supplementary Fig 1).

Following these voxelwise analyses, we performed a post-hoc regional analysis of the areas demonstrating SUVR group differences, in order to evaluate whether the effects emerging in the combined dataset could be similarly observed at each site independently (Table 4). This analysis revealed the presence of a statistically significant Site effect for all regions (p's<0.026), except for dmPFC (p=0.910) and SMA (p=0.078). It also revealed the presence of significant Site*Group interactions in SUVR for all regions examined (p's<0.047) except for dlPFC (p=0.072), dmPFC (p=0.237), frontoinsular cortex (p=0.362), pMCC (p=0.096), and SMA (p=0.624). The Cohen's d for the difference between FM patients and HC ranged between 0.58 and 1.04 at MGH and between 0.79 and 1.87 at KI (Table 4; Fig. 2), indicating medium or large effect size for all examined regions at both sites (Cohen, 1988), although the magnitude of the difference was generally larger for the KI study.

3.2.3 [^{11}C]PBR28 analysis: Agreement between SUVR and V_T (KI sample only).—

The regions identified in the voxelwise SUVR analysis displayed a large degree of spatial overlap with results from the V_T analysis. To visualize this, we created an image showing common regions identified in both analyses as significantly higher in FM patients. These regions included dlPFC, dmPFC, PCC, precuneus, S1/M1, SMA, and SPL (Fig. 3, left). In addition to this spatial agreement across analyses, we were able to evaluate the association across metrics in the KI participants, for whom both SUVR and V_T were available. Statistically significant positive correlations were observed for S1/M1 (r=0.453, p=0.039; Fig. 3, right), dmPFC (r=0.497, p=0.022), and PCC (r=0.491, p=0.024), whereas dlPFC (r=0.428, p=0.053), precuneus (r=0.384, p=0.085), and SPL (r=0.375, p=0.094) demonstrated only trend-level correlations.

3.3 [^{11}C]PBR28 analysis: Association with clinical variables (KI + MGH)

Within FM patients, an exploratory GLM analysis revealed that the scores of the Fatigue item of the ACR diagnostic criteria were significantly associated with SUVR in the aMCC ($F_{2,23}$=5.04, p=0.015, uncorrected) and pMCC ($F_{2,23}$=3.80, p=0.03, uncorrected), with

higher SUVR in patients reporting severe fatigue compared to those reporting slight/mild fatigue in both regions (p's≤0.01, uncorrected; Fig. 4). There were no significant associations between SUVR and any other clinical variable.

3.4 [^{11}C]-$_L$-deprenyl-D_2 analysis: Group differences (KI sample only)

Group comparisons of λk_3 values revealed no significant difference between FM patients and HC subjects, even when evaluated without correction for multiple comparisons, both within the regions demonstrating elevated [^{11}C]PBR28 SUVR (Fig. 5; p's≥0.53, uncorrected), as well as in any of the additional 23 anatomically defined ROIs, or in the whole brain or whole gray matter regions (p's≥0.53 uncorrected; Supplementary Table 3).

Of note, even in the small subset of 6 FM patients who received both [^{11}C]PBR28 and [^{11}C]-$_L$-deprenyl-D_2 scans, we were able to confirm elevated [^{11}C]PBR28 signal (p's≤0.007), but statistically indistinguishable [^{11}C]-$_L$-deprenyl-D_2 signal (p's≥0.63), compared to controls (Supplementary Figure 2).

4. DISCUSSION

The current study provides evidence of elevated TSPO binding, as measured with [^{11}C]PBR28 PET, in patients with fibromyalgia (FM) compared to healthy controls (HC). This marker of glial activation was increased in several brain regions implicated in FM pathology from previous neuroimaging studies. We also report positive associations between TSPO PET signal in several of these regions and subjective ratings of fatigue, one of the most common symptoms reported by FM patients (Clauw, 2014; Wolfe et al., 2011). Our observations are supportive of a role for neuroimmune/glial activation in FM pathology.

These results conform to a body of clinical data suggesting a possible association between neuroinflammation and FM. Several studies of FM patients demonstrated elevated CSF levels of molecules implicated in neuroglial signaling, such as fractalkine and IL-8 (Backryd et al., 2017; Kadetoff et al., 2012; Kosek et al., 2015). Furthermore, previous studies showed increased endogenous opioidergic tone in FM (Schrepf et al., 2016), which could be of relevance as opioid-induced hyperalgesia is associated with glial activation (Roeckel et al., 2016). In line with this evidence, some pharmacological treatments involving the opioid system and/or with putative inhibitory actions on glial cells are beneficial for FM. One example of this is low-dose naltrexone, an opioid antagonist, which is proposed to inhibit glial activation (Mattioli et al., 2010) and has been shown to have beneficial effects in FM (Younger and Mackey, 2009; Younger et al., 2009). Additionally, serotonin/noradrenaline reuptake inhibitors (SNRIs; e.g., duloxetine, milnacipran, etc.) are among the most commonly prescribed pharmacological treatments for FM, and show moderate effectiveness in reducing some FM symptoms (Welsch et al., 2018). While the primary mechanism of action of SNRIs is to normalize concentrations of endogenous monoamine neurotransmitters, which are thought to be imbalanced in FM (Albrecht et al., 2016; Kosek et al., 2016; Russell et al., 1992; Wood, 2008), one potential additional mechanism may be glial modulation, as both duloxetine (Yamashita et al., 2016) and milnacipran (Shadfar et al., 2018) attenuate microglial activation in animal models. Interestingly, among the regions demonstrating neuroimmune activation in our current study were the PCC/precuneus, a core

region of the default mode network, where post-treatment changes in pain related activation were specifically related to the degree of positive clinical response to milnacipran treatment in fibromyalgia patients (Jensen et al., 2014). Further studies are needed to better understand the specific cellular and molecular mechanisms of FM pharmacotherapies, and the potential role glial cell inhibition plays in their effectiveness.

The utility of TSPO as a marker of glial activation is supported by numerous preclinical and post-mortem studies. While TSPO is ubiquitously expressed by many cell types, it can be used as a sensitive marker of glial activation *in vitro* because it is dramatically upregulated in glial cells in the context of a neuroinflammatory response. TSPO upregulation has been colocalized with activated microglia and/or astrocytes across a spectrum of CNS disorders, including animal models of neuropathic pain (Liu et al., 2016; Wei et al., 2013), both animal MS models and human MS lesions (Abourbeh et al., 2012; Chen and Guilarte, 2006; Cosenza-Nashat et al., 2009), and both animal models of Alzheimer's disease (AD) and human post-mortem tissue (Cosenza-Nashat et al., 2009; Gulyas et al., 2009; James et al., 2017), among many others. The utility of TSPO as a marker of glial activation is further supported by numerous *in vivo* human PET imaging studies. In many of these, elevated TSPO PET signal is observed in brain regions where glial activation is known to occur. TSPO elevations have been documented in the primary motor cortex in Amyotrophic and Primary Lateral Sclerosis (Alshikho et al., 2016; Alshikho et al., 2018; Paganoni et al., 2018; Zurcher et al., 2015), in white matter or gray matter lesions in Multiple Sclerosis (Datta et al., 2017; Herranz et al., 2016), in amyloid positive regions in Alzheimer's Disease (Kreisl et al., 2013b; Parbo et al., 2017), and in the basal ganglia in Huntington's Disease (Lois et al., 2018). However, while a plethora of human and preclinical studies support TSPO as a glial marker, it is important to note that not all studies have detected TSPO upregulation in neuropathologies with a hypothesized inflammatory component. For instance, previous work showed no differences in TSPO PET signal in cocaine dependence (Narendran et al., 2014), and decreased signal in alcohol dependence (Hillmer et al., 2017; Kalk et al., 2017). In patients with psychosis, initial studies with first generation TSPO tracers showed an increase, whereas recent studies using second-generation radioligands are supportive of a decrease in TSPO levels (Plaven-Sigray et al., 2018). Thus, further work is needed to better assess the potential usefulness of TSPO as a means to image neuroinflammation, and the meaning of the observed TSPO signal changes, particularly in certain pathologies.

In addition, even in conditions for which TSPO may be more established as a marker of glial activation, the specific functional significance of its upregulation remains unclear, and represents an active area of investigation. Numerous preclinical studies show analgesic and anti-inflammatory effects of TSPO agonism, such as increased expression of anti-inflammatory IL-10 and other M2-related microglial genes, indicating that changes in TSPO expression might be an adaptive response to a homeostatic challenge (Bae et al., 2014; Liu et al., 2016; Wei et al., 2013). Similarly, recent *in vitro* human studies suggest that immune challenges induce TSPO upregulation in anti-inflammatory M2-like macrophages, and TSPO reduction in inflammatory M1-like macrophages (Narayan et al., 2017; Owen et al., 2017). We previously documented significantly higher CSF concentrations of IL-10 and other anti-inflammatory cytokines in FM patients, as opposed to a more classical (M1-like) pro-inflammatory CSF cytokine profile in patients with rheumatoid arthritis (RA; Kosek et

al., 2015; Lampa et al., 2012). Altogether, these observations suggest that the [^{11}C]PBR28 PET signal increases in FM patients might be reflective of a M2-like glial phenotype, although in the absence of PET tracers with a higher degree of phenotype specificity this remains speculative.

As mentioned above, elevated TSPO during a neuroinflammatory response may colocalize with both microglia and astrocytes, depending on the specific circumstances. As such, the exact cellular contributions of these glial subtypes to the TSPO PET signal are uncertain. In order to disambiguate the celluar specificity of the TSPO elevations observed in this study, a smaller sample of FM patients, partially overlapping with the sample scanned with [^{11}C]PBR28, was evaluated with [^{11}C]-$_{L}$-deprenyl-D_2, to quantify brain levels MAO-B. The expression of this protein in glial cells is thought to be predominantly, if not exclusively, within astrocytes, with little to no contribution from monocytes or microglia (Ekblom et al., 1994). For instance, MAO-B upregulation was found to be colocalized with reactive astrocytes in post-mortem tissues from patients with AD (Nakamura et al., 1990) and ALS (Ekblom et al., 1993; Ekblom et al., 1994), conditions that also demonstrate elevations in [^{11}C]-$_{L}$-deprenyl-D_2 PET signal (Johansson et al., 2007; Scholl et al., 2015). Because in the current study we observed no group differences in [^{11}C]-$_{L}$-deprenyl-D_2 binding, our data suggest that elevated [^{11}C]PBR28 signal in FM patients might be driven by activated microglia rather than astrocytes. Furthermore, the lack of group differences in [^{11}C]-$_{L}$-deprenyl-D_2 signal in any of the other anatomically-defined brain regions, including whole brain and whole gray matter, suggests that astrocyte activation may not be relevant to the FM pathophysiology.

In line with our current findings of elevated TSPO PET signal in FM patients, we have previously reported brain TSPO elevations in patients with another pain condition, chronic low back pain (Loggia et al., 2015b). In the cLBP study, we observed a different spatial pattern of glial activation that was localized to the thalamus and areas of the somatosensory and motor cortices consistent with the somatotopic representation of the back and leg, regions in which those participants experienced pain. In the FM patients, by contrast, we observed a pattern which was more spatially extendend, and involved only cortical areas. The larger cortical spread of neuroinflammation in FM patients compared to cLBP patients might be reflective of the differences in clinical presentation of these two patient groups, as the former report more widespread pain, and a higher incidence of cognitive issues and affective comorbidities (Clauw, 2014). Of note, the majority of FM patients also report low back pain but, unlike in our previous [^{11}C]PBR28 cLBP study, we did not observe statistically significant elevations in thalamic TSPO PET signal in FM, suggesting that similar pain symptoms in the two disorders may be mediated by distinct mechanisms. On the other hand, TSPO PET signal in the cingulate cortex, which in our FM patients was associated with fatigue scores, was also found to be elevated in patients with chronic fatigue syndrome/myalgic encephalomyelitis (CFS/ME; Nakatomi et al., 2014), suggesting glial activation in this region as a potential mechanism underlying pathological fatigue across different conditions.

Importantly, our results showed that elevated [^{11}C]PBR28 signal in FM, which was initially identified in the main analysis combining datasets from two different sites (KI+MGH), could

be observed within each site separately in follow-up analyses (Fig. 2). The reproducibility of the effects across sites strengthens confidence in the solidity of our observations. However, we also noticed that the effect sizes for the KI dataset were overall larger compared to those for the MGH dataset. This difference in magnitude of group differences between sites could be a result of several contributing factors, including differences in imaging procedures, e.g., different PET scanners, attenuation correction methodology, tracer injection parameters, tracer synthesis, etc. Additionally, patients from the KI site had significantly higher scores on several ACR items, including symptom severity and trouble thinking clearly (Table 2), and were less medicated (Table 3).

Finally, we observed an overlap in the spatial pattern of [^{11}C]PBR28 PET group differences between the SUVR and V_T analyses (Fig. 3), indicating that these analytical techniques may have similar abilities to detect regions exhibiting neuroinflammation in FM. This observation is in accordance with previous studies comparing [^{11}C]PBR28 metrics computed with (e.g., V_T, DVR) or without (e.g., SUVR) an arterial input function in different populations (Albrecht et al., 2017; Lyoo et al., 2015). While in the current study we also observed significant positive correlations between SUVR and V_T in several cortical regions, it should be noted that an association between these metrics has not been consistently observed in the literature (Matheson et al., 2017). A more thorough investigation of the relationship between SUVR and V_T is warranted to better understand this discrepancy across studies.

There are several caveats to take into consideration when interpreting results of the current study. In our voxelwise analyses, we implemented a cluster-forming threshold of $z > 2.3$, which has been criticized by some for being susceptible to false positives (Eklund et al., 2016). However, we were able to show elevations in [^{11}C]PBR28 signal independently for each study site, indicating that the effect is likely to be the result of a true physiological effect. Additionally, in the analyses evaluating the association between [^{11}C]PBR28 signal and clinical variables, no correction for multiple comparisons was utilized. While we feel that this exploratory approach is warranted, given that this is the first study demonstrating TSPO signal elevations in FM, the clinical significance of [^{11}C]PBR28 signal elevation in FM awaits further investigation. Furthermore, the ACR data for all KI patients and 2 MGH patients were acquired during the screening visit, but not at the scan visit. Though scores on this questionnaire show temporal stability, it is possible that scores for some patients may have changed between screening and scanning. Finally, the results of the [^{11}C]-$_L$-deprenyl-D_2 analysis should also be interpreted with caution. Importantly, the absence of a significant effect cannot be used as conclusive proof of no difference, especially with a small sample size as in the current study. Further analysis with larger samples will be thus needed to confirm that astrocytes do not have a key role in the pathophysiology of FM.

In conclusion, our work shows that brain levels of the glial marker, TSPO, as measured using [^{11}C]PBR28 PET imaging, are elevated in the cortex of FM patients relative to healthy controls. Furthermore, we found an association between the TSPO PET signal and fatigue, a predominant FM symptom. The lack of elevated [^{11}C]-$_L$-deprenyl-D_2 binding in FM may be viewed as support of an involvement of microglial, rather than astrocytic, activation. Future

studies will need to test whether glial modulation may be a viable therapeutic strategy for FM.

Supplementary Material

Refer to Web version on PubMed Central for supplementary material.

Acknowledgments

The authors would like to thank Grae Arabasz, Shiley Hsu, Regan Butterfield, Judit Sore, Patricia McCarthy, Marlene Wentworth, Jiaxuan (Jessie) Wang, Amy Kendall, Natacha Nortelus, and Atreyi Saha (MGH) and Carola Skärvinge, Maria Ahlsén, Karin Sahlander and Nina Knave (KI). We also thank the A. A. Martinos Center for Biomedical Imaging and the Stockholm Spine Center, Stockholm, Sweden for providing research facilities for the study and the staff for help with data collection. We are grateful to Lars Farde for engagement in designing and planning the study.

Funding

The study was supported by the following funding sources: International Association for the Study of Pain Early Career Award (MLL), DoD-W81XWH-14-1-0543 (MLL), R01-NS094306-01A1 (MLL), R01-NS095937-01A1 (MLL), R21-NS087472-01A1 (MLL), R01-AR064367 (VN, RRE), R01-AT007550 (VN), Martinos Center Pilot Grant for Postdoctoral Fellows (DSA), Harvard Catalyst Advance Imaging Pilot Grant (JMH), P41RR14075, 5T32EB13180 (T32 supporting DSA), and P41EB015896. The Swedish part of the study received funding from Stockholm County Council (EK), Swedish research Council (K2013-52X-22199-01-3 and 2016-01556) (EK), (2013–9306) (JL), the Swedish Rheumatism Association (EK) and Fibromyalgiförbundet (EK, DK). The research was also funded from the European Union Seventh Framework Programme (FP7/2007–2013) under grant agreement no.602919 (EK, JL) and from a donation from the Lundblad family (EK).

REFERENCES

Abourbeh G, Theze B, Maroy R, Dubois A, Brulon V, Fontyn Y, Dolle F, Tavitian B, Boisgard R, 2012 Imaging microglial/macrophage activation in spinal cords of experimental autoimmune encephalomyelitis rats by positron emission tomography using the mitochondrial 18 kDa translocator protein radioligand [(1)(8)F]DPA-714. J Neurosci 32, 5728–5736. [PubMed: 22539835]

Albrecht D, Ahmed S, Kettner N, Borra R, Cohen-Adad J, Deng H, Houle T, Opalacz A, Roth S, Melo MV, 2018 Neuroinflammation of the spinal cord and nerve roots in chronic radicular pain patients. Pain.

Albrecht DS, MacKie PJ, Kareken DA, Hutchins GD, Chumin EJ, Christian BT, Yoder KK, 2016 Differential dopamine function in fibromyalgia. Brain Imaging Behav 10, 829–839. [PubMed: 26497890]

Albrecht DS, Normandin MD, Shcherbinin S, Wooten DW, Schwarz AJ, Zurcher NR, Barth VN, Guehl NJ, Johnson-Akeju O, Atassi N, Veronese M, Turkheimer F, Hooker JM, Loggia ML, 2017 Pseudo-reference regions for glial imaging with (11)C-PBR28: investigation in two clinical cohorts. J Nucl Med.

Alshikho MJ, Zurcher NR, Loggia ML, Cernasov P, Chonde DB, Izquierdo Garcia D, Yasek JE, Akeju O, Catana C, Rosen BR, Cudkowicz ME, Hooker JM, Atassi N, 2016 Glial activation colocalizes with structural abnormalities in amyotrophic lateral sclerosis. Neurology 87, 2554–2561. [PubMed: 27837005]

Alshikho MJ, Zurcher NR, Loggia ML, Cernasov P, Reynolds B, Pijanowski O, Chonde DB, Izquierdo Garcia D, Mainero C, Catana C, Chan J, Babu S, Paganoni S, Hooker JM, Atassi N, 2018 Integrated MRI and [(11) C]-PBR28 PET Imaging in Amyotrophic Lateral sclerosis. Annals of neurology.

Backryd E, Tanum L, Lind AL, Larsson A, Gordh T, 2017 Evidence of both systemic inflammation and neuroinflammation in fibromyalgia patients, as assessed by a multiplex protein panel applied to the cerebrospinal fluid and to plasma. J Pain Res 10, 515–525. [PubMed: 28424559]

Bae KR, Shim HJ, Balu D, Kim SR, Yu SW, 2014 Translocator protein 18 kDa negatively regulates inflammation in microglia. J Neuroimmune Pharmacol 9, 424–437. [PubMed: 24687172]

Beck AT, Ward CH, Mendelson M, Mock J, Erbaugh J, 1961 An inventory for measuring depression. Archives of general psychiatry 4, 561–571. [PubMed: 13688369]

Bennett RM, Friend R, Jones KD, Ward R, Han BK, Ross RL, 2009 The Revised Fibromyalgia Impact Questionnaire (FIQR): validation and psychometric properties. Arthritis Res Ther 11, R120. [PubMed: 19664287]

Canat X, Carayon P, Bouaboula M, Cahard D, Shire D, Roque C, Le Fur G, Casellas P, 1993 Distribution profile and properties of peripheral-type benzodiazepine receptors on human hemopoietic cells. Life sciences 52, 107–118. [PubMed: 8380214]

Chen MK, Guilarte TR, 2006 Imaging the peripheral benzodiazepine receptor response in central nervous system demyelination and remyelination. Toxicol Sci 91, 532–539. [PubMed: 16554315]

Clauw DJ, 2014 Fibromyalgia: a clinical review. JAMA 311, 1547–1555. [PubMed: 24737367]

Clow A, Glover V, Sandler M, 1985 Triazolam, an anomalous benzodiazepine receptor ligand: in vitro characterization of alprazolam and triazolam binding. J Neurochem 45, 621–625. [PubMed: 2861251]

Cohen J, 1988 Statistical power analysis for the behavioral sciences. L. Erlbaum Associates, Hillsdale, N.J.

Collste K, Forsberg A, Varrone A, Amini N, Aeinehband S, Yakushev I, Halldin C, Farde L, Cervenka S, 2016 Test-retest reproducibility of [(11)C]PBR28 binding to TSPO in healthy control subjects. Eur J Nucl Med Mol Imaging 43, 173–183. [PubMed: 26293827]

Cosenza-Nashat M, Zhao ML, Suh HS, Morgan J, Natividad R, Morgello S, Lee SC, 2009 Expression of the translocator protein of 18 kDa by microglia, macrophages and astrocytes based on immunohistochemical localization in abnormal human brain. Neuropathol Appl Neurobiol 35, 306–328. [PubMed: 19077109]

Cselenyi Z, Olsson H, Farde L, Gulyas B, 2002 Wavelet-aided parametric mapping of cerebral dopamine D2 receptors using the high affinity PET radioligand [11C]FLB 457. Neuroimage 17, 47–60. [PubMed: 12482067]

Datta G, Colasanti A, Rabiner EA, Gunn RN, Malik O, Ciccarelli O, Nicholas R, Van Vlierberghe E, Van Hecke W, Searle G, Santos-Ribeiro A, Matthews PM, 2017 Neuroinflammation and its relationship to changes in brain volume and white matter lesions in multiple sclerosis. Brain 140, 2927–2938. [PubMed: 29053775]

Dehghan M, Schmidt-Wilcke T, Pfleiderer B, Eickhoff SB, Petzke F, Harris RE, Montoya P, Burgmer M, 2016 Coordinate-based (ALE) meta-analysis of brain activation in patients with fibromyalgia. Human brain mapping 37, 1749–1758. [PubMed: 26864780]

Dickens AM, Vainio S, Marjamaki P, Johansson J, Lehtiniemi P, Rokka J, Rinne J, Solin O, Haaparanta-Solin M, Jones PA, Trigg W, Anthony DC, Airas L, 2014 Detection of microglial activation in an acute model of neuroinflammation using PET and radiotracers 11C-(R)-PK11195 and 18F-GE-180. J Nucl Med 55, 466–472. [PubMed: 24516258]

Ekblom J, Jossan SS, Bergstrom M, Oreland L, Walum E, Aquilonius SM, 1993 Monoamine oxidase-B in astrocytes. Glia 8, 122–132. [PubMed: 8406673]

Ekblom J, Jossan SS, Oreland L, Walum E, Aquilonius SM, 1994 Reactive gliosis and monoamine oxidase B. Journal of neural transmission. Supplementum 41, 253–258.

Eklund A, Nichols TE, Knutsson H, 2016 Cluster failure: Why fMRI inferences for spatial extent have inflated false-positive rates. Proceedings of the National Academy of Sciences of the United States of America 113, 7900–7905. [PubMed: 27357684]

Flodin P, Martinsen S, Lofgren M, Bileviciute-Ljungar I, Kosek E, Fransson P, 2014 Fibromyalgia is associated with decreased connectivity between pain- and sensorimotor brain areas. Brain Connect 4, 587–594. [PubMed: 24998297]

Forsberg A, Cervenka S, Jonsson Fagerlund M, Rasmussen LS, Zetterberg H, Erlandsson Harris H, Stridh P, Christensson E, Granstrom A, Schening A, Dymmel K, Knave N, Terrando N, Maze M, Borg J, Varrone A, Halldin C, Blennow K, Farde L, Eriksson LI, 2017 The immune response of the human brain to abdominal surgery. Annals of neurology 81, 572–582. [PubMed: 28253549]

Fowler JS, Wang GJ, Logan J, Xie S, Volkow ND, MacGregor RR, Schlyer DJ, Pappas N, Alexoff DL, Patlak C, et al., 1995 Selective reduction of radiotracer trapping by deuterium substitution:

comparison of carbon-11-L-deprenyl and carbon-11-deprenyl-D2 for MAO B mapping. J Nucl Med 36, 1255–1262. [PubMed: 7790952]

Gehlert DR, Yamamura HI, Wamsley JK, 1985 Autoradiographic localization of "peripheral-type" benzodiazepine binding sites in the rat brain, heart and kidney. Naunyn-Schmiedeberg's archives of pharmacology 328, 454–460.

Gracely RH, Petzke F, Wolf JM, Clauw DJ, 2002 Functional magnetic resonance imaging evidence of augmented pain processing in fibromyalgia. Arthritis Rheum 46, 1333–1343. [PubMed: 12115241]

Gulyas B, Makkai B, Kasa P, Gulya K, Bakota L, Varszegi S, Beliczai Z, Andersson J, Csiba L, Thiele A, Dyrks T, Suhara T, Suzuki K, Higuchi M, Halldin C, 2009 A comparative autoradiography study in post mortem whole hemisphere human brain slices taken from Alzheimer patients and age-matched controls using two radiolabelled DAA1106 analogues with high affinity to the peripheral benzodiazepine receptor (PBR) system. Neurochem Int 54, 28–36. [PubMed: 18984021]

Gulyas B, Pavlova E, Kasa P, Gulya K, Bakota L, Varszegi S, Keller E, Horvath MC, Nag S, Hermecz I, Magyar K, Halldin C, 2011 Activated MAO-B in the brain of Alzheimer patients, demonstrated by [11C]-L-deprenyl using whole hemisphere autoradiography. Neurochem Int 58, 60–68. [PubMed: 21075154]

Harris RE, Clauw DJ, Scott DJ, McLean SA, Gracely RH, Zubieta JK, 2007 Decreased central mu-opioid receptor availability in fibromyalgia. J Neurosci 27, 10000–10006. [PubMed: 17855614]

Herranz E, Gianni C, Louapre C, Treaba CA, Govindarajan ST, Ouellette R, Loggia ML, Sloane JA, Madigan N, Izquierdo-Garcia D, Ward N, Mangeat G, Granberg T, Klawiter EC, Catana C, Hooker JM, Taylor N, Ionete C, Kinkel RP, Mainero C, 2016 Neuroinflammatory component of gray matter pathology in multiple sclerosis. Ann. Neurol 80, 776–790. [PubMed: 27686563]

Hillmer AT, Sandiego CM, Hannestad J, Angarita GA, Kumar A, McGovern EM, Huang Y, O'Connor KC, Carson RE, O'Malley SS, Cosgrove KP, 2017 In vivo imaging of translocator protein, a marker of activated microglia, in alcohol dependence. Molecular psychiatry 22, 1759–1766. [PubMed: 28242869]

Imaizumi M, Briard E, Zoghbi SS, Gourley JP, Hong J, Fujimura Y, Pike VW, Innis RB, Fujita M, 2008 Brain and whole-body imaging in nonhuman primates of [11C]PBR28, a promising PET radioligand for peripheral benzodiazepine receptors. Neuroimage 39, 1289–1298. [PubMed: 18024084]

Imaizumi M, Kim HJ, Zoghbi SS, Briard E, Hong J, Musachio JL, Ruetzler C, Chuang DM, Pike VW, Innis RB, Fujita M, 2007 PET imaging with [11C]PBR28 can localize and quantify upregulated peripheral benzodiazepine receptors associated with cerebral ischemia in rat. Neurosci Lett 411, 200–205. [PubMed: 17127001]

Izquierdo-Garcia D, Hansen AE, Forster S, Benoit D, Schachoff S, Furst S, Chen KT, Chonde DB, Catana C, 2014 An SPM8-based approach for attenuation correction combining segmentation and nonrigid template formation: application to simultaneous PET/MR brain imaging. J Nucl Med 55, 1825–1830. [PubMed: 25278515]

James ML, Belichenko NP, Shuhendler AJ, Hoehne A, Andrews LE, Condon C, Nguyen TV, Reiser V, Jones P, Trigg W, Rao J, Gambhir SS, Longo FM, 2017 [(18)F]GE-180 PET Detects Reduced Microglia Activation After LM11A-31 Therapy in a Mouse Model of Alzheimer's Disease. Theranostics 7, 1422–1436. [PubMed: 28529627]

Jensen KB, Kosek E, Petzke F, Carville S, Fransson P, Marcus H, Williams SC, Choy E, Giesecke T, Mainguy Y, Gracely R, Ingvar M, 2009 Evidence of dysfunctional pain inhibition in Fibromyalgia reflected in rACC during provoked pain. Pain 144, 95–100. [PubMed: 19410366]

Jensen KB, Petzke F, Carville S, Choy E, Fransson P, Gracely RH, Vitton O, Marcus H, Williams SC, Ingvar M, Kosek E, 2014 Segregating the cerebral mechanisms of antidepressants and placebo in fibromyalgia. The journal of pain : official journal of the American Pain Society 15, 1328–1337. [PubMed: 25283470]

Jensen KB, Petzke F, Carville S, Fransson P, Marcus H, Williams SC, Choy E, Mainguy Y, Gracely R, Ingvar M, Kosek E, 2010 Anxiety and depressive symptoms in fibromyalgia are related to poor perception of health but not to pain sensitivity or cerebral processing of pain. Arthritis Rheum 62, 3488–3495. [PubMed: 20617526]

Jensen KB, Srinivasan P, Spaeth R, Tan Y, Kosek E, Petzke F, Carville S, Fransson P, Marcus H, Williams SC, Choy E, Vitton O, Gracely R, Ingvar M, Kong J, 2013 Overlapping structural and functional brain changes in patients with long-term exposure to fibromyalgia pain. Arthritis Rheum 65, 3293–3303. [PubMed: 23982850]

Johansson A, Engler H, Blomquist G, Scott B, Wall A, Aquilonius SM, Langstrom B, Askmark H, 2007 Evidence for astrocytosis in ALS demonstrated by [11C](L)-deprenyl-D2 PET. Journal of the neurological sciences 255, 17–22. [PubMed: 17346749]

Jucaite A, Svenningsson P, Rinne JO, Cselenyi Z, Varnas K, Johnstrom P, Amini N, Kirjavainen A, Helin S, Minkwitz M, Kugler AR, Posener JA, Budd S, Halldin C, Varrone A, Farde L, 2015 Effect of the myeloperoxidase inhibitor AZD3241 on microglia: a PET study in Parkinson's disease. Brain 138, 2687–2700. [PubMed: 26137956]

Kadetoff D, Lampa J, Westman M, Andersson M, Kosek E, 2012 Evidence of central inflammation in fibromyalgia-increased cerebrospinal fluid interleukin-8 levels. J Neuroimmunol 242, 33–38. [PubMed: 22126705]

Kalk NJ, Guo Q, Owen D, Cherian R, Erritzoe D, Gilmour A, Ribeiro AS, McGonigle J, Waldman A, Matthews P, Cavanagh J, McInnes I, Dar K, Gunn R, Rabiner EA, Lingford-Hughes AR, 2017 Decreased hippocampal translocator protein (18 kDa) expression in alcohol dependence: a [(11)C]PBR28 PET study. Transl Psychiatry 7, e996. [PubMed: 28072413]

Kalk NJ, Owen DR, Tyacke RJ, Reynolds R, Rabiner EA, Lingford-Hughes AR, Parker CA, 2013 Are prescribed benzodiazepines likely to affect the availability of the 18 kDa translocator protein (TSPO) in PET studies? Synapse 67, 909–912. [PubMed: 23666806]

Kanegawa N, Collste K, Forsberg A, Schain M, Arakawa R, Jucaite A, Lekander M, Olgart Hoglund C, Kosek E, Lampa J, Halldin C, Farde L, Varrone A, Cervenka S, 2016 In vivo evidence of a functional association between immune cells in blood and brain in healthy human subjects. Brain Behav Immun 54, 149–157. [PubMed: 26820224]

Kolb A, Wehrl HF, Hofmann M, Judenhofer MS, Eriksson L, Ladebeck R, Lichy MP, Byars L, Michel C, Schlemmer HP, Schmand M, Claussen CD, Sossi V, Pichler BJ, 2012 Technical performance evaluation of a human brain PET/MRI system. European radiology 22, 1776–1788. [PubMed: 22752524]

Kosek E, Altawil R, Kadetoff D, Finn A, Westman M, Le Maitre E, Andersson M, Jensen-Urstad M, Lampa J, 2015 Evidence of different mediators of central inflammation in dysfunctional and inflammatory pain--interleukin-8 in fibromyalgia and interleukin-1 beta in rheumatoid arthritis. J Neuroimmunol 280, 49–55. [PubMed: 25773155]

Kosek E, Martinsen S, Gerdle B, Mannerkorpi K, Lofgren M, Bileviciute-Ljungar I, Fransson P, Schalling M, Ingvar M, Ernberg M, Jensen KB, 2016 The translocator protein gene is associated with symptom severity and cerebral pain processing in fibromyalgia. Brain Behav Immun 58, 218–227. [PubMed: 27448744]

Kragel PA, Kano M, Van Oudenhove L, Ly HG, Dupont P, Rubio A, Delon-Martin C, Bonaz BL, Manuck SB, Gianaros PJ, Ceko M, Reynolds Losin EA, Woo CW, Nichols TE, Wager TD, 2018 Generalizable representations of pain, cognitive control, and negative emotion in medial frontal cortex. Nature neuroscience 21, 283–289. [PubMed: 29292378]

Kreisl WC, Jenko KJ, Hines CS, Lyoo CH, Corona W, Morse CL, Zoghbi SS, Hyde T, Kleinman JE, Pike VW, McMahon FJ, Innis RB, Biomarkers Consortium, P.E.T.R.P.T., 2013a A genetic polymorphism for translocator protein 18 kDa affects both in vitro and in vivo radioligand binding in human brain to this putative biomarker of neuroinflammation. J. Cereb. Blood Flow Metab. 33, 53–58. [PubMed: 22968319]

Kreisl WC, Lyoo CH, McGwier M, Snow J, Jenko KJ, Kimura N, Corona W, Morse CL, Zoghbi SS, Pike VW, McMahon FJ, Turner RS, Innis RB, Biomarkers Consortium, P.E.T.R.P.T., 2013b In vivo radioligand binding to translocator protein correlates with severity of Alzheimer's disease. Brain 136, 2228–2238. [PubMed: 23775979]

Kuchinad A, Schweinhardt P, Seminowicz DA, Wood PB, Chizh BA, Bushnell MC, 2007 Accelerated brain gray matter loss in fibromyalgia patients: premature aging of the brain? J Neurosci 27, 4004–4007. [PubMed: 17428976]

Lampa J, Westman M, Kadetoff D, Agreus AN, Le Maitre E, Gillis-Haegerstrand C, Andersson M, Khademi M, Corr M, Christianson CA, Delaney A, Yaksh TL, Kosek E, Svensson CI, 2012

Peripheral inflammatory disease associated with centrally activated IL-1 system in humans and mice. Proceedings of the National Academy of Sciences of the United States of America 109, 12728–12733. [PubMed: 22802629]

Lavisse S, Guillermier M, Herard AS, Petit F, Delahaye M, Van Camp N, Ben Haim L, Lebon V, Remy P, Dolle F, Delzescaux T, Bonvento G, Hantraye P, Escartin C, 2012 Reactive astrocytes overexpress TSPO and are detected by TSPO positron emission tomography imaging. J Neurosci 32, 10809–10818. [PubMed: 22875916]

Liu X, Liu H, Xu S, Tang Z, Xia W, Cheng Z, Li W, Jin Y, 2016 Spinal translocator protein alleviates chronic neuropathic pain behavior and modulates spinal astrocyte-neuronal function in rats with L5 spinal nerve ligation model. Pain 157, 103–116. [PubMed: 26307860]

Logan J, Fowler JS, Volkow ND, Wang GJ, MacGregor RR, Shea C, 2000 Reproducibility of repeated measures of deuterium substituted [11C]L-deprenyl ([11C]L-deprenyl-D2) binding in the human brain. Nucl Med Biol 27, 43–49. [PubMed: 10755644]

Logan J, Fowler JS, Volkow ND, Wolf AP, Dewey SL, Schlyer DJ, MacGregor RR, Hitzemann R, Bendriem B, Gatley SJ, et al., 1990 Graphical analysis of reversible radioligand binding from time-activity measurements applied to [N-11C-methyl]-(−)-cocaine PET studies in human subjects. J Cereb Blood Flow Metab 10, 740–747. [PubMed: 2384545]

Loggia ML, Berna C, Kim J, Cahalan CM, Gollub RL, Wasan AD, Harris RE, Edwards RR, Napadow V, 2014 Disrupted brain circuitry for pain-related reward/punishment in fibromyalgia. Arthritis Rheumatol 66, 203–212. [PubMed: 24449585]

Loggia ML, Berna C, Kim J, Cahalan CM, Martel MO, Gollub RL, Wasan AD, Napadow V, Edwards RR, 2015a The lateral prefrontal cortex mediates the hyperalgesic effects of negative cognitions in chronic pain patients. The journal of pain : official journal of the American Pain Society 16, 692–699. [PubMed: 25937162]

Loggia ML, Chonde DB, Akeju O, Arabasz G, Catana C, Edwards RR, Hill E, Hsu S, Izquierdo-Garcia D, Ji RR, Riley M, Wasan AD, Zurcher NR, Albrecht DS, Vangel MG, Rosen BR, Napadow V, Hooker JM, 2015b Evidence for brain glial activation in chronic pain patients. Brain 138(pt. 3), 604–615. [PubMed: 25582579]

Lois C, Gonzalez I, Izquierdo-Garcia D, Zurcher NR, Wilkens P, Loggia ML, Hooker JM, Rosas HD, 2018 Neuroinflammation in Huntington's Disease: New Insights with (11)C-PBR28 PET/MRI. ACS chemical neuroscience.

Lyoo CH, Ikawa M, Liow JS, Zoghbi SS, Morse CL, Pike VW, Fujita M, Innis RB, Kreisl WC, 2015 Cerebellum can serve as a pseudo-reference region in alzheimer disease to detect neuroinflammation measured with PET radioligand binding to translocator protein. J Nucl Med 56, 701–706. [PubMed: 25766898]

Matheson GJ, Plaven-Sigray P, Forsberg A, Varrone A, Farde L, Cervenka S, 2017 Assessment of simplified ratio-based approaches for quantification of PET [(11)C]PBR28 data. EJNMMI research 7, 58. [PubMed: 28733954]

Mattioli TA, Milne B, Cahill CM, 2010 Ultra-low dose naltrexone attenuates chronic morphine-induced gliosis in rats. Mol Pain 6, 22. [PubMed: 20398374]

Mirzaei N, Tang SP, Ashworth S, Coello C, Plisson C, Passchier J, Selvaraj V, Tyacke RJ, Nutt DJ, Sastre M, 2016 In vivo imaging of microglial activation by positron emission tomography with [(11)C]PBR28 in the 5XFAD model of Alzheimer's disease. Glia 64, 993–1006. [PubMed: 26959396]

Montague K, Malcangio M, 2017 The therapeutic potential of targeting chemokine signalling in the treatment of chronic pain. J Neurochem 141, 520–531. [PubMed: 27973687]

Nakamura S, Kawamata T, Akiguchi I, Kameyama M, Nakamura N, Kimura H, 1990 Expression of monoamine oxidase B activity in astrocytes of senile plaques. Acta Neuropathol 80, 419–425. [PubMed: 2239154]

Nakatomi Y, Mizuno K, Ishii A, Wada Y, Tanaka M, Tazawa S, Onoe K, Fukuda S, Kawabe J, Takahashi K, Kataoka Y, Shiomi S, Yamaguti K, Inaba M, Kuratsune H, Watanabe Y, 2014 Neuroinflammation in Patients with Chronic Fatigue Syndrome/Myalgic Encephalomyelitis: An (1)(1)C-(R)-PK11195 PET Study. J Nucl Med 55, 945–950. [PubMed: 24665088]

Napadow V, Harris RE, 2014 What has functional connectivity and chemical neuroimaging in fibromyalgia taught us about the mechanisms and management of 'centralized' pain? Arthritis Res Ther 16, 425. [PubMed: 25606591]

Narayan N, Mandhair H, Smyth E, Dakin SG, Kiriakidis S, Wells L, Owen D, Sabokbar A, Taylor P, 2017 The macrophage marker translocator protein (TSPO) is down-regulated on pro-inflammatory 'M1' human macrophages. PLoS One 12, e0185767. [PubMed: 28968465]

Narendran R, Lopresti BJ, Mason NS, Deuitch L, Paris J, Himes ML, Kodavali CV, Nimgaonkar VL, 2014 Cocaine abuse in humans is not associated with increased microglial activation: an 18-kDa translocator protein positron emission tomography imaging study with [11C]PBR28. J Neurosci 34, 9945–9950. [PubMed: 25057196]

Oaklander AL, Herzog ZD, Downs HM, Klein MM, 2013 Objective evidence that small-fiber polyneuropathy underlies some illnesses currently labeled as fibromyalgia. Pain 154, 2310–2316. [PubMed: 23748113]

Owen DR, Howell OW, Tang SP, Wells LA, Bennacef I, Bergstrom M, Gunn RN, Rabiner EA, Wilkins MR, Reynolds R, Matthews PM, Parker CA, 2010 Two binding sites for [3H]PBR28 in human brain: implications for TSPO PET imaging of neuroinflammation. J Cereb Blood Flow Metab 30, 1608–1618. [PubMed: 20424634]

Owen DR, Narayan N, Wells L, Healy L, Smyth E, Rabiner EA, Galloway D, Williams JB, Lehr J, Mandhair H, Peferoen LA, Taylor PC, Amor S, Antel JP, Matthews PM, Moore CS, 2017 Pro-inflammatory activation of primary microglia and macrophages increases 18 kDa translocator protein expression in rodents but not humans. J Cereb Blood Flow Metab 37, 2679–2690. [PubMed: 28530125]

Owen DR, Yeo AJ, Gunn RN, Song K, Wadsworth G, Lewis A, Rhodes C, Pulford DJ, Bennacef I, Parker CA, StJean PL, Cardon LR, Mooser VE, Matthews PM, Rabiner EA, Rubio JP, 2012 An 18-kDa translocator protein (TSPO) polymorphism explains differences in binding affinity of the PET radioligand PBR28. J. Cereb. Blood Flow Metab. 32, 1–5. [PubMed: 22008728]

Paganoni S, Alshikho MJ, Zurcher NR, Cernasov P, Babu S, Loggia ML, Chan J, Chonde DB, Garcia DI, Catana C, Mainero C, Rosen BR, Cudkowicz ME, Hooker JM, Atassi N, 2018 Imaging of glia activation in people with primary lateral sclerosis. NeuroImage. Clinical 17, 347–353. [PubMed: 29159046]

Parbo P, Ismail R, Hansen KV, Amidi A, Marup FH, Gottrup H, Braendgaard H, Eriksson BO, Eskildsen SF, Lund TE, Tietze A, Edison P, Pavese N, Stokholm MG, Borghammer P, Hinz R, Aanerud J, Brooks DJ, 2017 Brain inflammation accompanies amyloid in the majority of mild cognitive impairment cases due to Alzheimer's disease. Brain 140, 2002–2011. [PubMed: 28575151]

Plaven-Sigray P, Matheson GJ, Collste K, Ashok AH, Coughlin JM, Howes OD, Mizrahi R, Pomper MG, Rusjan P, Veronese M, Wang Y, Cervenka S, 2018 Positron Emission Tomography Studies of the Glial Cell Marker Translocator Protein in Patients With Psychosis: A Meta-analysis Using Individual Participant Data. Biological psychiatry.

Puma C, Danik M, Quirion R, Ramon F, Williams S, 2001 The chemokine interleukin-8 acutely reduces Ca(2+) currents in identified cholinergic septal neurons expressing CXCR1 and CXCR2 receptor mRNAs. J Neurochem 78, 960–971. [PubMed: 11553670]

Roeckel LA, Le Coz GM, Gaveriaux-Ruff C, Simonin F, 2016 Opioid-induced hyperalgesia: Cellular and molecular mechanisms. Neuroscience 338, 160–182. [PubMed: 27346146]

Rupprecht R, Papadopoulos V, Rammes G, Baghai TC, Fan J, Akula N, Groyer G, Adams D, Schumacher M, 2010 Translocator protein (18 kDa) (TSPO) as a therapeutic target for neurological and psychiatric disorders. Nature reviews. Drug discovery 9, 971–988. [PubMed: 21119734]

Russell IJ, Vaeroy H, Javors M, Nyberg F, 1992 Cerebrospinal fluid biogenic amine metabolites in fibromyalgia/fibrositis syndrome and rheumatoid arthritis. Arthritis Rheum 35, 550–556. [PubMed: 1374252]

Scholl M, Carter SF, Westman E, Rodriguez-Vieitez E, Almkvist O, Thordardottir S, Wall A, Graff C, Langstrom B, Nordberg A, 2015 Early astrocytosis in autosomal dominant Alzheimer's disease measured in vivo by multi-tracer positron emission tomography. Scientific reports 5, 16404. [PubMed: 26553227]

Schreiber KL, Loggia ML, Kim J, Cahalan CM, Napadow V, Edwards RR, 2017 Painful After-Sensations in Fibromyalgia are Linked to Catastrophizing and Differences in Brain Response in the Medial Temporal Lobe. The journal of pain : official journal of the American Pain Society 18, 855–867. [PubMed: 28300650]

Schrepf A, Harper DE, Harte SE, Wang H, Ichesco E, Hampson JP, Zubieta JK, Clauw DJ, Harris RE, 2016 Endogenous opioidergic dysregulation of pain in fibromyalgia: a PET and fMRI study. Pain 157, 2217–2225. [PubMed: 27420606]

Shackman AJ, Salomons TV, Slagter HA, Fox AS, Winter JJ, Davidson RJ, 2011 The integration of negative affect, pain and cognitive control in the cingulate cortex. Nat Rev Neurosci 12, 154–167. [PubMed: 21331082]

Shadfar S, Kim YG, Katila N, Neupane S, Ojha U, Bhurtel S, Srivastav S, Jeong GS, Park PH, Hong JT, Choi DY, 2018 Neuroprotective Effects of Antidepressants via Upregulation of Neurotrophic Factors in the MPTP Model of Parkinson's Disease. Molecular neurobiology 55, 554–566. [PubMed: 27975170]

Sturm S, Forsberg A, Nave S, Stenkrona P, Seneca N, Varrone A, Comley RA, Fazio P, Jamois C, Nakao R, Ejduk Z, Al-Tawil N, Akenine U, Halldin C, Andreasen N, Ricci B, 2017 Positron emission tomography measurement of brain MAO-B inhibition in patients with Alzheimer's disease and elderly controls after oral administration of sembragiline. Eur J Nucl Med Mol Imaging 44, 382–391. [PubMed: 27633250]

Sullivan MJ, Bishop SR, Pivik J, 1995 The pain catastrophizing scale: development and validation. Psychological assessment 7, 524.

Toth M, Little P, Arnberg F, Haggkvist J, Mulder J, Halldin C, Gulyas B, Holmin S, 2016 Acute neuroinflammation in a clinically relevant focal cortical ischemic stroke model in rat: longitudinal positron emission tomography and immunofluorescent tracking. Brain Struct Funct 221, 1279–1290. [PubMed: 25601153]

Tzourio-Mazoyer N, Landeau B, Papathanassiou D, Crivello F, Etard O, Delcroix N, Mazoyer B, Joliot M, 2002 Automated anatomical labeling of activations in SPM using a macroscopic anatomical parcellation of the MNI MRI single-subject brain. Neuroimage 15, 273–289. [PubMed: 11771995]

Uceyler N, Sommer C, 2013 Objective evidence that small-fiber polyneuropathy underlies some illnesses currently labeled as fibromyalgia. Pain 154, 2569.

Wamsley JK, Longlet LL, Hunt ME, Mahan DR, Alburges ME, 1993 Characterization of the binding and comparison of the distribution of benzodiazepine receptors labeled with [3H]diazepam and [3H]alprazolam. Neuropsychopharmacology : official publication of the American College of Neuropsychopharmacology 8, 305–314. [PubMed: 8390266]

Wei XH, Wei X, Chen FY, Zang Y, Xin WJ, Pang RP, Chen Y, Wang J, Li YY, Shen KF, Zhou LJ, Liu XG, 2013 The upregulation of translocator protein (18 kDa) promotes recovery from neuropathic pain in rats. J. Neurosci 33, 1540–1551. [PubMed: 23345228]

Welsch P, Uceyler N, Klose P, Walitt B, Hauser W, 2018 Serotonin and noradrenaline reuptake inhibitors (SNRIs) for fibromyalgia. Cochrane Database Syst Rev 2, CD010292. [PubMed: 29489029]

Wolfe F, Clauw DJ, Fitzcharles MA, Goldenberg DL, Hauser W, Katz RS, Mease P, Russell AS, Russell IJ, Winfield JB, 2011 Fibromyalgia criteria and severity scales for clinical and epidemiological studies: a modification of the ACR Preliminary Diagnostic Criteria for Fibromyalgia. J Rheumatol 38, 1113–1122. [PubMed: 21285161]

Wolfe F, Smythe HA, Yunus MB, Bennett RM, Bombardier C, Goldenberg DL, Tugwell P, Campbell SM, Abeles M, Clark P, et al., 1990 The American College of Rheumatology 1990 Criteria for the Classification of Fibromyalgia. Report of the Multicenter Criteria Committee. Arthritis Rheum 33, 160–172. [PubMed: 2306288]

Wood PB, 2008 Role of central dopamine in pain and analgesia. Expert Rev Neurother 8, 781–797. [PubMed: 18457535]

Yamashita T, Yamamoto S, Zhang J, Kometani M, Tomiyama D, Kohno K, Tozaki-Saitoh H, Inoue K, Tsuda M, 2016 Duloxetine Inhibits Microglial P2X4 Receptor Function and Alleviates Neuropathic Pain after Peripheral Nerve Injury. PLoS One 11, e0165189. [PubMed: 27768754]

Younger J, Mackey S, 2009 Fibromyalgia symptoms are reduced by low-dose naltrexone: a pilot study. Pain medicine 10, 663–672. [PubMed: 19453963]

Younger JW, Zautra AJ, Cummins ET, 2009 Effects of naltrexone on pain sensitivity and mood in fibromyalgia: no evidence for endogenous opioid pathophysiology. PLoS One 4, e5180. [PubMed: 19365548]

Zurcher NR, Loggia ML, Lawson R, Chonde DB, Izquierdo-Garcia D, Yasek JE, Akeju O, Catana C, Rosen BR, Cudkowicz ME, Hooker JM, Atassi N, 2015 Increased in vivo glial activation in patients with amyotrophic lateral sclerosis: assessed with [(11)C]-PBR28. Neuroimage Clin. 7, 409–414. [PubMed: 25685708]

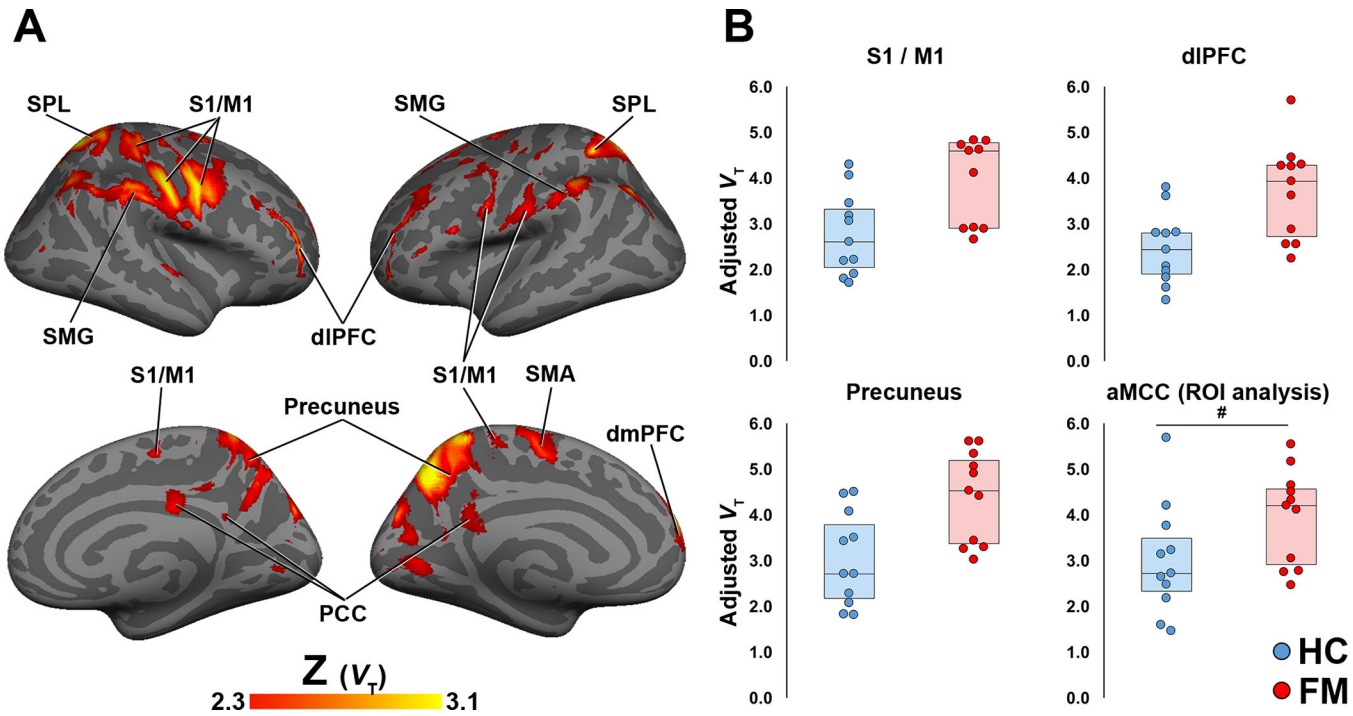

Figure 1. Voxelwise group differences in [^{11}C]PBR28 V_T.

A: Surface projection maps displaying areas with significantly elevated [^{11}C]PBR28 V_T in FM patients compared to controls (FM – n=11; HC – n=11) in voxelwise analyses (KI-only sample). *B*: average ± standard deviation V_T extracted from several regions. The S1/M1, dLPFC and precuneus data were extracted from the clusters identified as statistically significant in the voxelwise V_T analysis. For these regions, the plots are displayed for illustrative purposes only, and the level of statistical significance noted for each plot reflects that of the voxelwise analyses. For the aMCC, the data was extracted from a region, independently identified based on the results of the SUVR voxelwise analysis (see Fig. 2). The level of statistical significance noted for this region reflects the result of a region-of-interest analysis.

SPL – superior parietal lobule, S1 – primary somatosensory cortex, M1 – primary motor cortex, SMG – supramarginal gyrus, dlPFC – dorsolateral prefrontal cortex, SMA – supplementary motor area, PCC – posterior cingulate cortex, dmPFC – dorsomedial prefrontal cortex. The barplots for S1/M1, dlPFC and Precuneus are for illustrative purposes. The barplot for aMCC illustrates an ROI analysis (p=0.071)

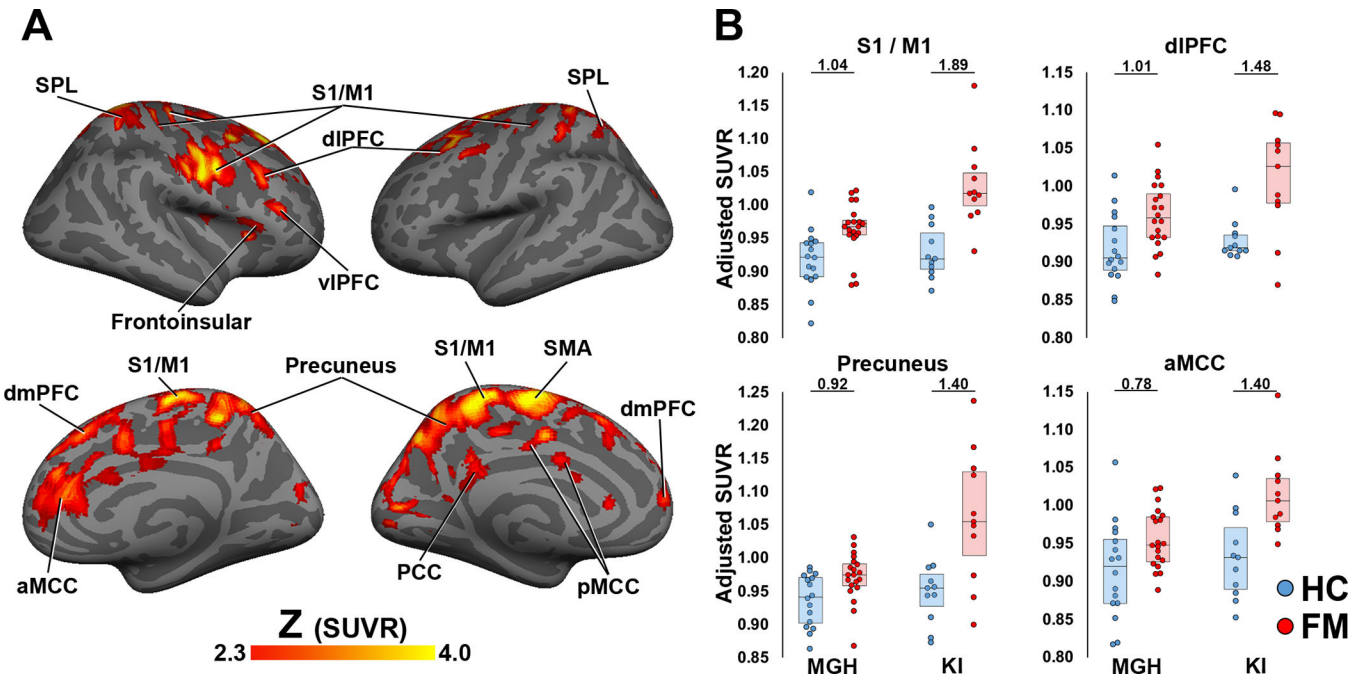

Figure 2. Voxelwise group differences in [^{11}C]PBR28 SUVR

A: Surface projection maps displaying areas with significantly elevated [^{11}C]PBR28 SUVR in FM patients compared to controls (FM – n=31; HC – n=27), in voxelwise analyses (KI +MGH sample).

B: average ± standard deviation SUVR extracted from several of the clusters identified as statistically significant in the voxelwise SUVR analysis. Data from individual research sites (MGH or KI) are displayed separately, and the number above each ROI pairing corresponds to the effect size (Cohen's *d*) of PET signal differences between FM patients and controls for each site. These data show that overall SUVR group differences, while larger for the KI dataset, are elevated in FM patients compared to controls in both datasets when evaluated independently. pMCC – posterior middle cingulate cortex, aMCC – anterior middle cingulate cortex. All data have been adjusted for genotype and injected dose.

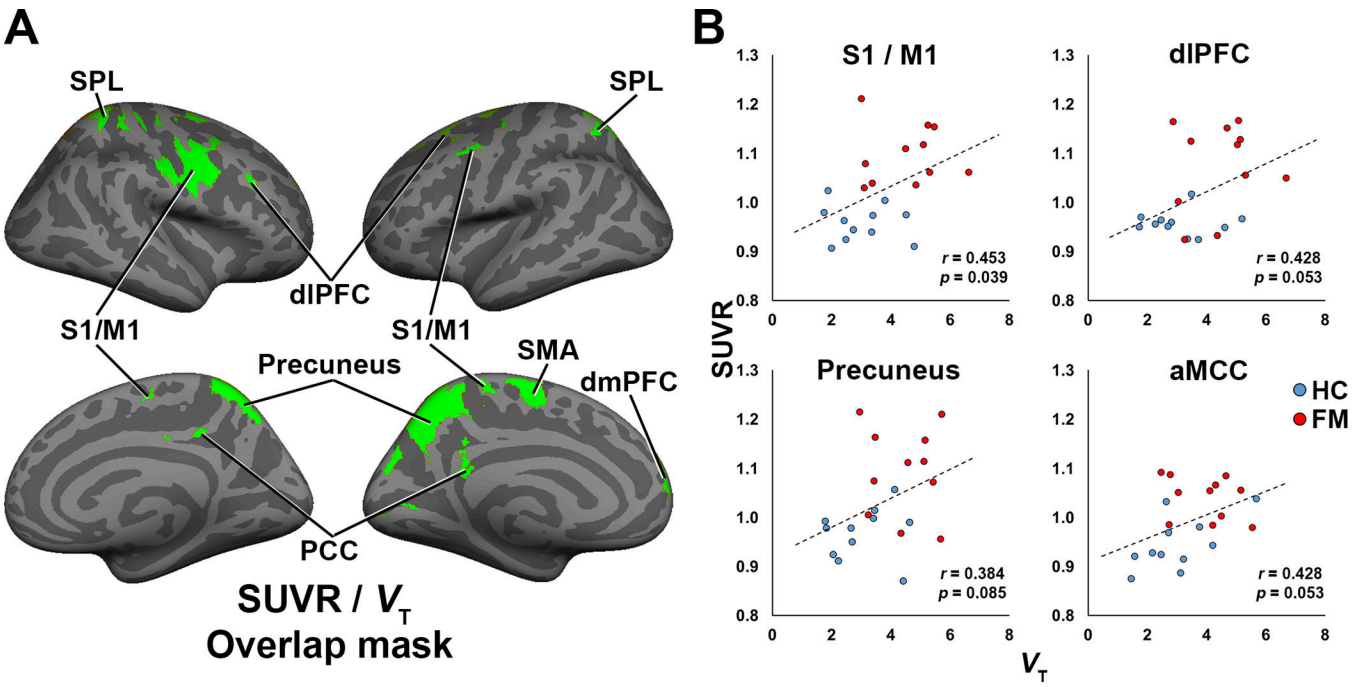

Figure 3. Agreement between SUVR and V_T analyses

A: Surface projection displaying the regions showing elevated PET signal across both SUVR (KI+MGH combined dataset) and V_T (KI-only) analyses. *B*: Cross-correlations between SUVR and V_T, extracted from regions identified in the overlap mask or, for the aMCC, from the SUVR analyses, in FM patients and HC from the KI site.

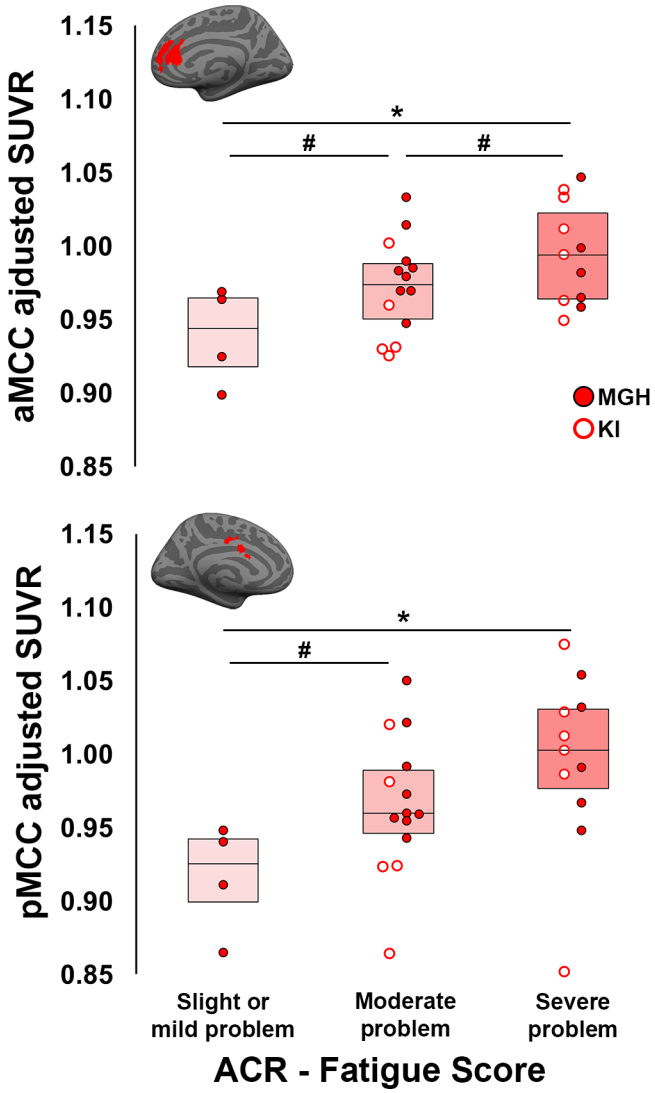

Figure 4. Associations between [^{11}C]PBR28 SUVR and clinical variables

Significant differences in [^{11}C]PBR28 SUVR in the aMCC (top) and pMCC (bottom) between FM patients reporting different severity of fatigue on the ACR 2011 questionnaire. Surface projections of individual ROIs are displayed in red above the plots. All data have been adjusted for *TSPO* genotype.

* - Significant difference in post-hoc tests between FM patients reporting different levels of fatigue severity (p<0.01)

- Trend-level difference in post-hoc tests between FM patients reporting different levels of fatigue severity (p<0.10)

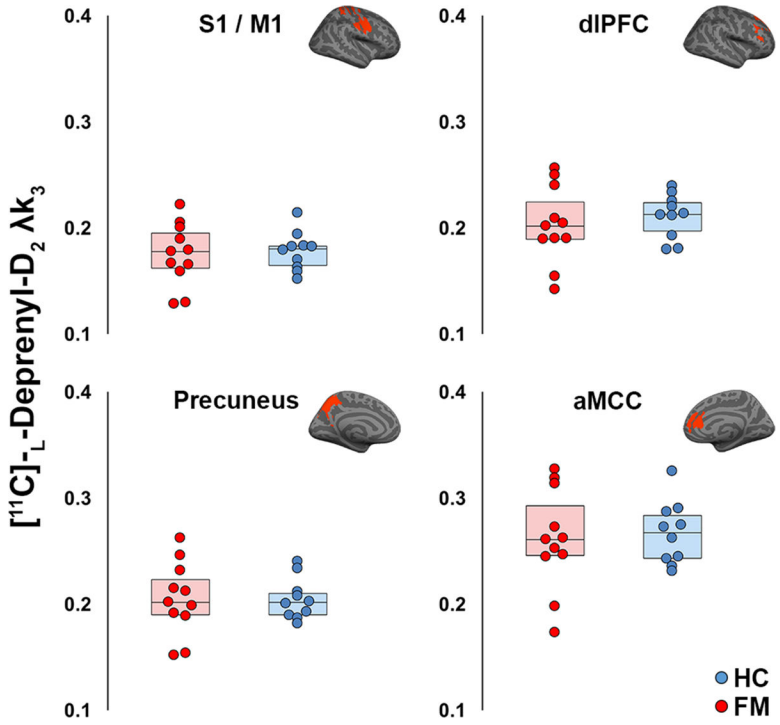

Figure 5. Absence of group differences in [^{11}C]-$_L$-deprenyl-D_2 λk_3.

Four representative regions showing significant group differences in the [^{11}C]PBR28 SUVR analysis (Fig 2) show no differences in [^{11}C]-$_L$-deprenyl-D_2 λk_3 ($p \geq 0.53$ uncorrected). Surface projections of individual regions are displayed in red above the plots.

Table 1.

Participant characteristics

	Massachusetts General Hospital [^{11}C]PBR28		**Karolinska Institutet [^{11}C]PBR28**		**Karolinska Institutet [^{11}C]-$_L$-deprenyl-D_2**	
	FM (*n*=20)	**HC (*n*=16)**	**FM (*n*=11)[1]**	**HC (*n*=11)**	**FM (*n*=11)[2]**	**HC (*n*=11)**
Age (years)	48.0 ± 12	50.2 ± 13	51.8 ± 8.6	51.5 ± 9.0	51.5 ± 8.2	51.0 ± 7.0
Sex	18F; 2M	14F; 2M	11F	11F	11F	11F
TSPO polymorphism	14 HAB; 6 MAB	10 HAB; 6 MAB	8 HAB; 3 MAB	8 HAB; 3 MAB	N/A	
BMI	30.0 ± 5.7*	23.6 ± 3.6	24.5 ± 3.7	23.1 ± 2.0	24.5 ± 3.0	22.3 ± 1.8
Injected dose (MBq)	505 ± 40	457 ± 57	385 ± 71	416 ± 40	366 ± 45	364 ± 46
Specific activity (GBq/μmol)	71.8 ± 26	77.4 ± 30	239 ± 74	306 ± 195	213 ± 82	193 ± 105
Injected mass (μg)	2.78 ± 1.1	2.32 ± 0.8	0.61 ± 0.21	0.60 ± 0.34	0.36 ± 0.13	0.48 ± 0.30

[1] Six of the FM subjects receiving a [^{11}C]PBR28 scan also received a [^{11}C]-L-deprenyl-D_2 scan

[2] [^{11}C]-L-deprenyl-D_2 data from one FM subject was not used due to a technical issue during arterial blood collection.

* Significantly different from controls within-cohort, $p < 0.05$

Table 2.

FM patient clinical characteristics: [^{11}C]PBR28 analysis.

	Massachusetts General Hospital [^{11}C]PBR28	**Karolinska Institutet [^{11}C]PBR28**	**Karolinska Institutet [^{11}C]-$_L$-deprenyl-D_2**
N	20	11	11
Current VAS pain	37.8 ± 23	47.2 ± 15	42.9 ± 16
FIQ pain	5.15 ± 2.0	5.82 ± 1.2	5.80 ± 1.1
FIQ stiffness	6.35 ± 2.1	6.18 ± 2.4	6.13 ± 2.3
FIQ depression	2.75 ± 2.6	3.36 ± 3.3	3.35 ± 3.0
FIQ anxiety	3.55 ± 2.9	4.55 ± 3.4	4.62 ± 3.4
ACR total	18.6 ± 4.3	24.7 ± 3.3 **	25.5 ± 3.2
ACR symptom severity	7.61 ± 1.9	9.09 ± 1.8 *	9.00 ± 1.8
ACR widespread pain index	10.9 ± 3.3	16.1 ± 2.0 **	16.5 ± 1.7
ACR fatigue	2.06 ± 0.7	2.55 ± 0.5 #	2.64 ± 0.5
ACR trouble thinking	1.61 ± 0.9	2.64 ± 0.5 **	2.18 ± 0.8
ACR waking tired	2.11 ± 0.6	2.27 ± 0.5	2.64 ± 0.5
BDI	12.5 ± 9.2	14.9 ± 6.1	12.2 ± 5.7
PCS	17.5 ± 9.1	17.2 ± 11	17.5 ± 11

FIQ - Fibromyalgia Impact Questionnaire; ACR - 2011 modifications of the American College of Rheumatology diagnostic criteria for fibromyalgia; BDI - Beck Depression Inventory; PCS - Pain Catastrophizing Scale

* Significant difference between KI and MGH FM patients from the [^{11}C]PBR28 datasets, $p < 0.05$

** Significant difference between KI and MGH FM patients from the [^{11}C]PBR28 datasets, $p < 0.01$

Trend-level difference between KI and MGH FM patients from the [^{11}C]PBR28 datasets, $p < 0.10$

Table 3.

FM patient medications

Medication	Massachusetts General Hospital	Karolinska Institutet [^{11}C]PBR28	Karolinska Institutet [^{11}C]-$_{L}$-deprenyl-D_2
N	20	11	11
NSAIDs	6	5	2
Acetominophen (paracetamol)	2	6	4
Muscle relaxant	8	2	1
Sleep medication	2	2	3
SNRI	6	0	0
Anticonvulsant	2	0	0
Opioid	1	0	0
Benzodiazepines	9	0	0
Tricyclic antidepressant	6	0	0

Table 4.

Site-specific comparison of SUVR

Region	Effect of Site	Group*site interaction	MGH - FM vs. HC Effect size	KI - FM vs. HC Effect size
aMCC	**$F_{1,52}$ = 13.2, p = 0.001**	**$F_{1,52}$ = 4.16, p = 0.047**	0.78	1.46
dlPFC	**$F_{1,52}$ = 9.01, p = 0.004**	*$F_{1,52}$ = 3.38, p = 0.072*	1.01	1.48
dmPFC	$F_{1,52}$ = 0.01, p = 0.910	$F_{1,52}$ = 1.43, p = 0.237	0.74	1.70
Frontoinsular cortex	**$F_{1,52}$ = 5.22, p = 0.026**	$F_{1,52}$ = 0.85, p = 0.362	0.74	1.27
S1/M1	**$F_{1,52}$ = 18.1, p < 0.001**	**$F_{1,52}$ = 8.94, p = 0.004**	1.04	1.89
pMCC	**$F_{1,52}$ = 71.2, p < 0.001**	*$F_{1,52}$ = 2.88, p = 0.096*	0.83	0.79
PCC	**$F_{1,52}$ = 115, p < 0.001**	**$F_{1,52}$ = 14.7, p < 0.001**	0.58	1.12
Precuneus	**$F_{1,52}$ = 25.7, p < 0.001**	**$F_{1,52}$ = 12.7, p < 0.001**	0.92	1.40
SMA	*$F_{1,52}$ = 3.22, p = 0.078*	$F_{1,52}$ = 0.24, p = 0.624	1.02	1.19
SPL	**$F_{1,52}$ = 10.8, p = 0.002**	**$F_{1,52}$ = 13.5, p < 0.001**	0.82	1.71

Statistically significant results are displayed **in bold**, statistical tests exhibiting trend-level results are displayed *in italics*.

aMCC - anterior middle cingulate cortex, dmPFC - dorsomedial prefrontal cortex, dlPFC - dorsolateral prefrontal cortex, S1 - primary somatosensory cortex, M1 - primary motor cortex, pMCC - posterior middle cingulate cortex, PCC - posterior cingulate cortex, SMA - supplementary motor area, SPL - superior parietal lobule.